iScience

CellPress
OPEN ACCESS

Article

Multi-targeted loss of the antigen presentation molecule MR1 during HSV-1 and HSV-2 infection

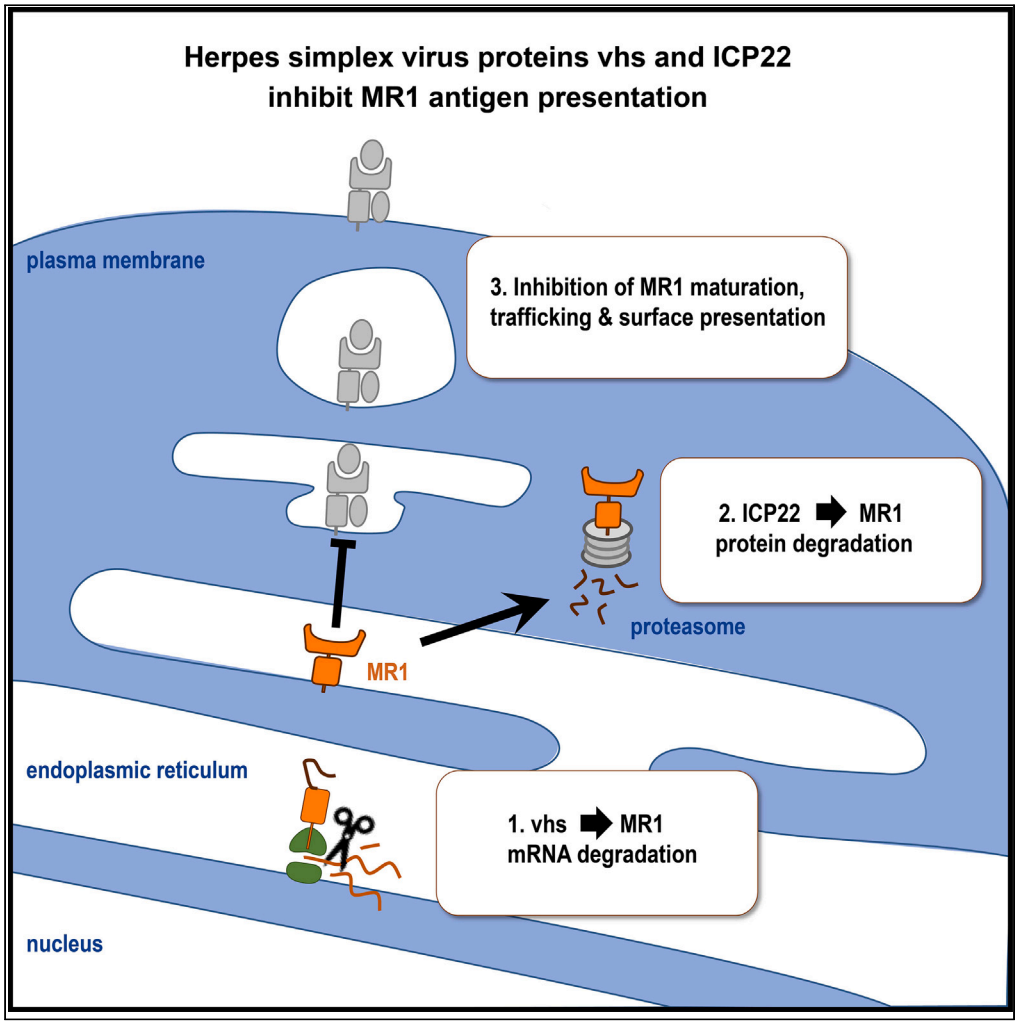

Carolyn Samer, Hamish E.G. McWilliam, Brian P. McSharry, ..., Jose A. Villadangos, Allison Abendroth, Barry Slobedman

barry.slobedman@sydney.edu.au

Highlights

HSV-1 virion host shutoff (vhs) RNase protein degrades MR1 transcripts

HSV-1 ICP22 protein targets MR1 for proteasomal degradation

HSV-2 downregulation of MR1 transcripts and protein mirrors HSV-1 modulation

Samer et al., iScience 27, 108801
February 16, 2024
https://doi.org/10.1016/j.isci.2024.108801

iScience

CellPress
OPEN ACCESS

Article

Multi-targeted loss of the antigen presentation molecule MR1 during HSV-1 and HSV-2 infection

Carolyn Samer,[1] Hamish E.G. McWilliam,[2,3] Brian P. McSharry,[1,4] Thilaga Velusamy,[5] James G. Burchfield,[6,7] Richard J. Stanton,[8] David C. Tscharke,[5] Jamie Rossjohn,[8,9] Jose A. Villadangos,[2,3] Allison Abendroth,[1,10] and Barry Slobedman[1,10,11,*]

SUMMARY

The major histocompatibility complex (MHC), Class-I-related (MR1) molecule presents microbiome-synthesized metabolites to Mucosal-associated invariant T (MAIT) cells, present at sites of herpes simplex virus (HSV) infection. During HSV type 1 (HSV-1) infection there is a profound and rapid loss of MR1, in part due to expression of unique short 3 protein. Here we show that virion host shutoff RNase protein downregulates MR1 protein, through loss of MR1 transcripts. Furthermore, a third viral protein, infected cell protein 22, also downregulates MR1, but not classical MHC-I molecules. This occurs early in the MR1 trafficking pathway through proteasomal degradation. Finally, HSV-2 infection results in the loss of MR1 transcripts, and intracellular and surface MR1 protein, comparable to that seen during HSV-1 infection. Thus HSV coordinates a multifaceted attack on the MR1 antigen presentation pathway, potentially protecting infected cells from MAIT cell T cell receptor-mediated detection at sites of primary infection and reactivation.

INTRODUCTION

Mucosal-associated invariant T (MAIT) cells are a tissue-resident and circulating memory T cell population that play key roles monitoring and responding to changes in the integrity of mucosal and barrier sites.[1–4] MAIT cells are pleiotropic innate-like T cells due to their expression of multiple transcription factors including promyelocytic leukemia zinc finger (PLZF),[5] their restricted repertoire of T cell receptors (TCRs), and activation through TCR-dependent and TCR-independent mechanisms.[6–10] Through TCR binding, MAIT cells recognize bacterial or fungal-sourced intermediates from the vitamin B biosynthesis pathway presented by the major histocompatibility complex (MHC), Class-I-related (MR1) molecule.[11] This allows MAIT cells to detect specific perturbations in the metabolome resulting from changes in the composition or location of the microbiome and pathogens.

Unlike classical T cells, MAIT cells can be activated by cytokines and Toll-like receptor (TLR) agonists that can also arise from diverse viral infections. Indeed, there is a growing appreciation of the importance of MAIT cell protection against viral infections including influenza A virus,[9] hepatitis C[12] and HIV-1.[13] MAIT cells are more abundant in the blood during dengue virus, correlating with disease severity,[12] while during early HIV infection blood and mucosal MAIT cells are activated and expanded, potentially responding to increased microbial translocation.[14] However in many viral infections including human T lymphotropic virus type 1,[15] influenza A virus,[10,12] hepatitis B virus,[16–19] hepatitis C virus,[12,20,21] hepatitis D virus,[18] chronic HIV,[22–25] and SARS-CoV-2,[26,27] circulating and tissue-resident MAIT cells are reduced in number, often expressing an exhausted phenotype.

MAIT TCR-mediated signaling in the absence of other markers of infection drives a Th17 tissue repair phenotype.[28,29] Although MAIT cells express a pro-inflammatory Th1 signature in response to TCR-independent factors, sustained activation with concurrent proliferation and targeted cytotoxicity requires the addition of TCR signaling.[1,30–32] While there is no evidence that viruses synthesize MR1 ligands, it is clear that viruses such as the human herpesviruses modulate the MR1-TCR MAIT cell axis.[33] Recent studies have also confirmed that riboflavin availability enhances MAIT cell protective responses to influenza A virus infections in mice[34] and inhibits entry of flaviviruses.[35] Herpesviruses establish a primary infection in the skin, lungs, orofacial, and genital mucosa, at sites colonized by MR1 ligand producing bacteria and monitored by

[1]Infection, Immunity and Inflammation, School of Medical Sciences, Faculty of Medicine and Health, and the Charles Perkins Centre, The University of Sydney, Camperdown, NSW, Australia
[2]Department of Microbiology and Immunology, Peter Doherty Institute for Infection and Immunity, The University of Melbourne, Melbourne, VIC, Australia
[3]Department of Biochemistry and Pharmacology, Bio21 Molecular Science and Biotechnology Institute, The University of Melbourne, Parkville, VIC, Australia
[4]School of Dentistry and Medical Sciences, Faculty of Science and Health, Charles Sturt University, Wagga Wagga, NSW, Australia
[5]John Curtin School of Medical Research, Australian National University, Canberra, ACT, Australia
[6]Charles Perkins Centre, The University of Sydney, Sydney, NSW, Australia
[7]School of Life and Environmental Sciences, University of Sydney, Sydney, NSW, Australia
[8]Division of Infection & Immunity, School of Medicine, Cardiff University, Cardiff, Wales
[9]Infection and Immunity Program, Department of Biochemistry and Molecular Biology, Biomedicine Discovery Institute, Monash University, Clayton, VIC, Australia
[10]These authors contributed equally
[11]Lead contact
*Correspondence: barry.slobedman@sydney.edu.au
https://doi.org/10.1016/j.isci.2024.108801

immune cell populations including MAIT cells. During primary lytic infection, virally induced disruptions at these barrier sites could increase MR1 antigen availability, driving the early activation arm of resident MAIT cells, with consequent TCR-mediated cytolysis of virally infected host cells. The synergistic MAIT cell activation associated with antiviral cytokines combined with this TCR signal would enhance the pro-inflammatory response of MAIT cells, a result that could strongly impact viral replication and transmission efficiency. Furthermore, a subset of MAIT cells respond to surface MR1 in the absence of microbial ligands, promoting T helper like functionality, including dendritic cell (DC) maturation.[36] In all these scenarios, disabling the MR1-TCR response would represent an advantage to viral survival.

We previously reported that herpes simplex virus type 1 (HSV-1), human cytomegalovirus (HCMV), and varicella zoster virus (VZV) all downregulate MR1 expression.[37–39] During HSV-1 infection, substantial loss of MR1 protein is detected during early infection, predominantly from the immature protein accumulating in the endoplasmic reticulum (ER) awaiting exogenous ligand.[37] Although pre-existing surface MR1 remains protected from HSV-1-induced loss, there is a substantial reduction in new surface MR1 resulting from depletion of the ER pool. While the viral kinase unique short (US) 3 and homolog open reading frame (ORF) 66 are implicated in MR1 inhibition in HSV-1 and VZV infections respectively, viruses lacking their expression fail to fully rescue the loss,[37,38] suggesting that additional viral products contribute to this suppression of MR1 expression.

HSV encodes approximately 84 viral gene products, which are expressed in a three-step immediate-early (IE), early (E), and late (L) sequential cascade.[40] IE products, which are synthesized immediately post release of the viral DNA into the host's nucleus, inhibit critical antiviral functions and promote pro-viral gene transcription and protein synthesis.[41–43] Here we provide evidence that one of these products, namely ICP22, contributes to the loss of ER-resident MR1 through proteasomal degradation. In contrast, a second IE protein, ICP47, which blocks peptide presentation by MHC-I molecules to classical T cells, does not play an apparent role in MR1 modulation. In addition, an HSV-1 late-expressed protein, the virion host shutoff (vhs) RNase protein encoded by the unique long (UL) 41 gene, contributes to the loss of MR1 protein through the downregulation of MR1 transcripts. We also report that a third alphaherpesvirus, HSV-2, modulates MR1 protein, replicating the HSV-1-mediated loss of immature MR1 and ligand-dependent modulation of antigen-bound surface molecules. Together these results expand the number of viruses that modulate this non-classical antigen presentation molecule and reveal that HSV-1 encodes multiple mechanisms to produce this immunomodulatory effect.

RESULTS

TAP inhibitor ICP47 modulates MHC-I but not MR1 antigen presentation

Loss of cellular MR1 is detectible within 4 h of HSV-1 infection in epithelial cells,[37] implicating one of the five IE proteins expressed immediately post viral entry. We have previously established that the IE E3 ubiquitin ligase protein ICP0 is not responsible for the loss of MR1 protein during HSV-1 infection.[37] A second IE protein, ICP47, is well characterized for its ability to inhibit classical MHC-I antigen presentation. ICP47 inhibits the transporter associated with antigen processing (TAP) protein dimer, thus preventing the delivery of peptides across the ER membrane into the lumen for loading into the MHC-I antigenic cleft.[41,44,45] TAP is part of the peptide loading complex (PLC) which can stabilize two antigen-presentation molecules simultaneously.[46] Components of the PLC contribute to MR1 stability and antigen loading in the ER[47]; consequently viral interference may indirectly impact MR1 stability.

To test whether expression of ICP47 during infection impacts MR1 antigen presentation, ARPE-19 epithelial cells were infected with HSV-1 KOS strain and ICP47 null mutant ICP47del[48] and analyzed by flow cytometry. Equivalent surface expression of the late viral glycoprotein gC was detected at 6 h post infection (p.i.) in the cells infected with both parental and mutant viruses (Figure 1A) confirming that deletion of the non-essential ICP47 protein had no impact on expression kinetics at this early time point. As expected, compared to mock-infected cells, surface MHC-I expression was downregulated by the parental virus, but not the mutant virus (Figure 1B), recapitulating the role ICP47 plays in the early loss of surface MHC-I.[49,50]

Increased surface MR1 associated with acetyl-6-formylpterin (Ac-6-FP) ligand-induced maturation and plasma membrane trafficking can be detected after 2 h, and peaks around 8 h post treatment.[51] In order to examine the effect of an IE viral gene on both total cellular MR1 and surface MR1, ARPE-19 cells transduced to express MR1-GFP[37] were treated with Ac-6-FP ligand 3 h p.i., after substantial IE gene expression,[52] and then harvested 3 h later. Both viruses invoked a similar loss of total MR1 as detected by the GFP signal (Figure 1C); however, consistent with previous reports, no loss of surface MR1 was evident at this early time point.[37] In cells similarly infected but treated with ligand 4 h prior to staining at 18 h p.i., a time point associated with complete gene expression and high yield of viral progeny,[53] the strong loss of both total and surface MR1 was again comparable in the parental and mutant infected cells (Figure 1D). Given the lack of rescue of total or surface MR1 by ICP47del at both early and late time points, this suggests that inhibition of TAP functionality by ICP47 does not interfere with PLC-mediated stability of MR1 in the ER and consequently does not contribute to the loss of MR1 during HSV-1 infection.

ICP22 viral protein promotes proteasomal degradation of MR1

The three remaining IE proteins, ICP4, ICP22, and ICP27, use multiple mechanisms to initiate and promote viral gene expression, at the expense of cellular expression, through interactions with cellular transcription and translation machinery. ICP22 is broadly characterized as a pro-viral *trans* regulator, without which viral replication is severely attenuated and viral progeny contain reduced amounts of some glycoproteins.[54] ICP22 is attributed with diverse roles during HSV-1 replication including the recruitment of cellular chaperones into nuclear virus enriched chaperone enhanced (VICE) domains adjacent to the viral replication centers,[55–57] modulation of RNA polymerase (pol) II,[58–61] and modulation of cell cycling.[62,63] Of particular interest, ICP22 may act as a J-protein co-chaperone, interacting with cellular Hsc70 protein to manage misfolded proteins.[57] In addition, HSV-2 ICP22 E3 ubiquitin ligase functionality is responsible for ubiquitination, and subsequent

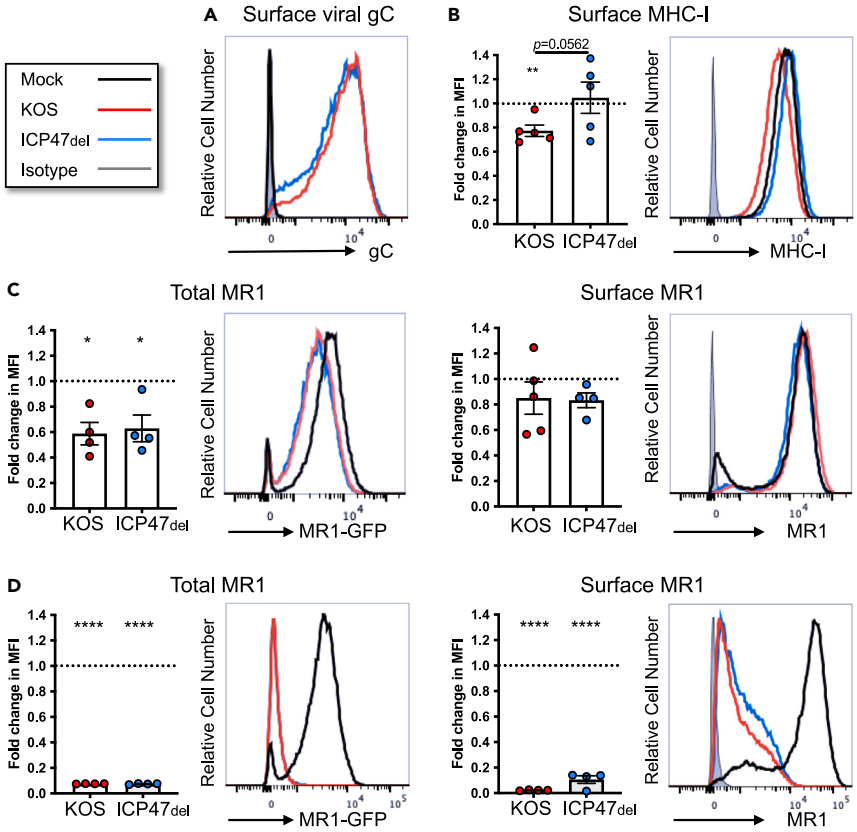

Figure 1. HSV-1 ICP47 deletion mutant fails to rescue loss of MR1

(A) ARPE-19 cells were mock (black), HSV-1 strain KOS (red), or ICP47del mutant lacking expression of ICP47 (blue) infected (MOI 3) in parallel. Cells were harvested at 6 h p.i. and stained for viral glycoprotein gC or matching isotype control (gray) and analyzed by flow cytometry. Histograms representative of two independent experiments.

(B–D) ARPE-19 MR1-GFP cells were mock (black), HSV-1 strain KOS (red), or ICP47del (blue) infected in parallel.

(B and C) Cells were treated with Ac-6-FP (5 μM) at 3 h p.i. before harvesting at 6 h p.i.

(D) or treated at 14 h p.i., before harvesting at 18 h p.i. Cells were stained for surface MHC-I (B) or surface MR1 (C, D) or matching isotype control (gray) and analyzed by flow cytometry. Fold change in MFI of infected cells relative to mock-infected cells (dotted black line) is represented as mean ± SEM. Statistical significance was calculated by paired Student's *t* test *p < 0.05, **p < 0.005, ****p < 0.0001. Analysis of 4 or 5 independent experiments.

degradation, of several signal transducer proteins in the type 1 interferon signaling pathway.[64] Consequently, ICP22 qualified as an interesting candidate for MR1 modulation.

To assess the impact of ICP22 expression on endogenous MR1 surface expression, the US1 gene from HSV-1 strain F was cloned into the pCDH_EF1-MCS-T2A-copGFP plasmid (pSY10) upstream of a T2A ribosomal skip sequence, thus facilitating the independent translation of GFP from the same transcript as a marker of successful transfection. 293T cells transfected with either parental (pSY10) or the US1 expressing (pSY10-ICP22) plasmid were treated with Ac-6-FP ligand 6 h prior to harvesting at 28 h p.i., at which point GFP was detectible in a subset of cells. The fold change in surface MHC-I and MR1 was calculated in GFP^+ cells compared to non-transfected GFP^- cells within the same sample. No difference in surface MR1 or MHC-I was associated with transfection of the parental plasmid compared to mock-infected cells (Figure 2A). Expression of ICP22 however resulted in a marked reduction in surface MR1 expression. By contrast MHC-I was instead upregulated in the ICP22-expressing cells suggesting a differential effect of ICP22 on these related antigen presenting molecules.

A second protein, US1.5, is translated from the US1 gene; however, there is uncertainty regarding which of the in-frame start codons initiates the carboxyl-terminant molecule.[58,65,66] During viral infection both ICP22 and US1.5 are expressed; though the latter only accumulates at later time points under the control of the US3 and UL13 viral kinases.[66]

Both HSV-1 strain F ICP22 and US1.5 from codon 171[60,66] were cloned with an N-terminal FLAG tag[58] into the replication-incompetent pAdZ5-C5 adenovirus vector.[67] ARPE-19 MR1-GFP cells were infected with parental (RAd-Ctrl), ICP22 (RAd-ICP22)-, or US1.5 (RAd-US1.5)-expressing virus, at an MOI of 100, for detection of total cellular MR1 and surface MR1 and MHC-I by flow cytometry. Cells were optionally treated with Ac-6-FP ligand 4 h (Post) prior to harvesting at 44 h p.i. At this time point mild adenovirus-associated cytopathic effect was detected, reflecting successful adenovirus infection; however, there was minimal cell death associated with overexpression of the viral genes that was evident at later time points. In parallel, ARPE-19 cells expressing MR1 were similarly infected and harvested to detect the size of the

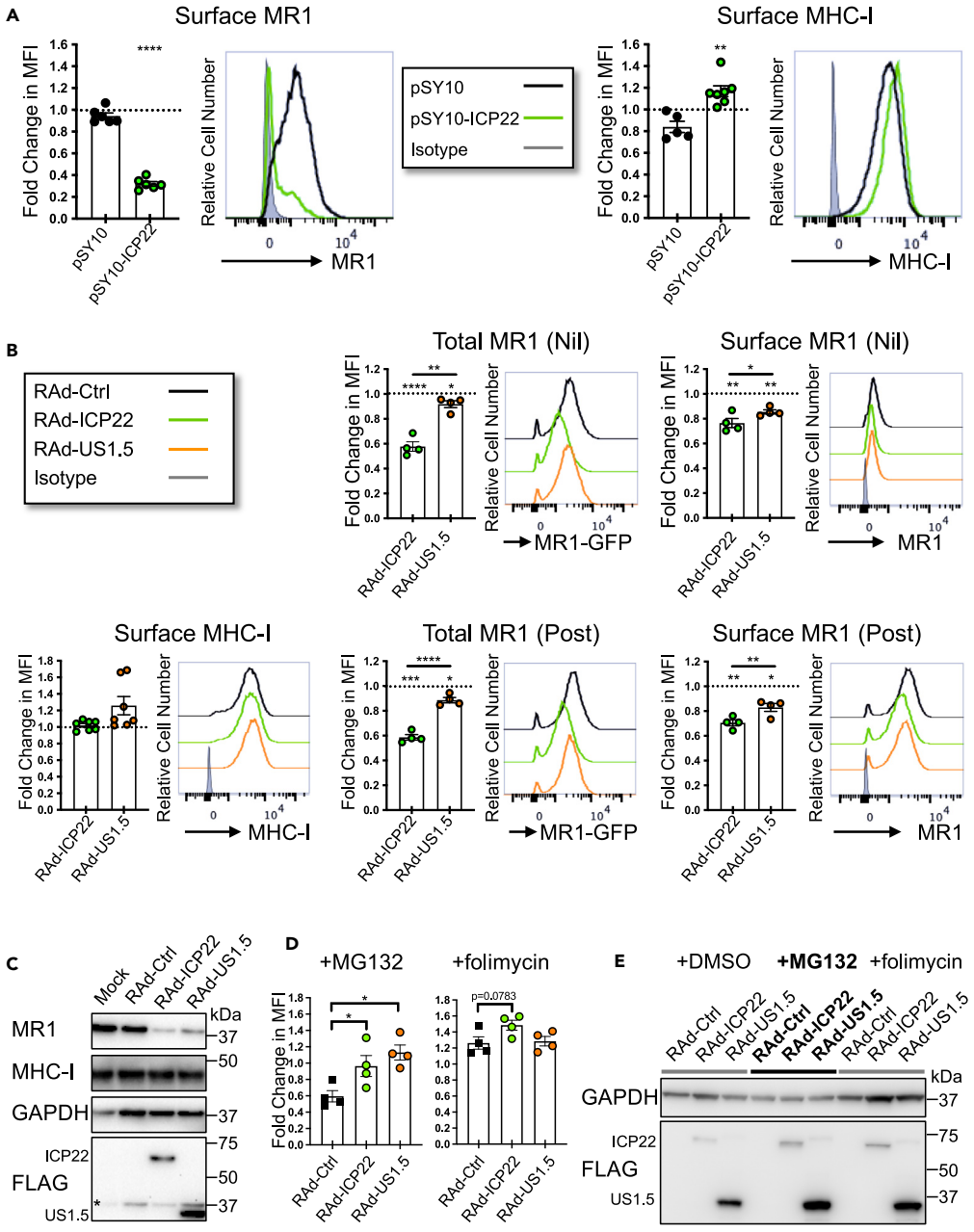

Figure 2. ICP22 expression modulates loss of total and surface MR1

(A) 293T cells were transfected with a plasmid encoding either GFP alone (pSY10, black) or GFP and HSV-1 US1 gene (pSY10-ICP22, green). Cells were treated with Ac-6-FP (5 μM) 22 h post transfection and harvested 6 h later. Cells were stained for surface MR1 or MHC-I and analyzed by flow cytometry. Fold change in MFI relative to GFP^- cells (dotted line) within each sample was calculated and is represented as mean ± SEM. Statistical significance compared to pSY10 was evaluated by Welch's unpaired t test $^{**}p < 0.005$, $^{****}p < 0.0001$. Analysis of 6 or 7 independent experiments.

(B) ARPE-19 MR1-GFP cells were infected with RAd-Ctrl adenovirus (black or dotted line) or RAd-Ctrl modified to encode HSV-1 US1 gene (RAd-ICP22, green) or HSV-1 US1.5 gene (RAd-US1.5, orange), MOI 100. Cells were left untreated (Nil) or treated with Ac-6-FP (5 μM) for 4 h prior to harvesting at 44 h p.i. (Post). Cells were stained for surface MR1, MHC-I, or matching isotype control (gray) and analyzed by flow cytometry. Fold change in MFI of live infected cells relative to RAd-Ctrl with matching ligand treatment is represented as mean ± SEM. Statistical significance was calculated by paired Student's *t* test, $^{*}p < 0.05$, $^{**}p < 0.005$, $^{****}p < 0.0001$. Analysis of 4 independent experiments.

(C) ARPE-19 MR1 cells were infected with RAd-Ctrl, RAd-ICP22, or RAd-US1.5 or mock infected. Cells were harvested at 44 h p.i. and lysates were separated by gel electrophoresis before immunoblotting for MR1, MHC-I, GAPDH, and FLAG to detect expression of the viral gene. Faint GAPDH band from prior probe denoted *.

Figure 2. *Continued*

(D and E) ARPE-19 MR1-GFP cells were infected with RAd-Ctrl (black), RAd-ICP22 (green), or RAd-US1.5 (orange), MOI 100 for 46 h. Cells were treated with proteasomal inhibitor MG132 (5 μM), lysosomal inhibitor folimycin (50 nM), or DMSO vehicle control (1:400) for a further 16 h prior to harvest and analysis by (D) flow cytometry or (E) immunoblot.

(D) Fold change of total MR1 (GFP) was detected by flow cytometry (inhibitor:DMSO) in live cells for each adenovirus and is represented as mean ± SEM. Statistical significance was calculated by paired Student's *t* test, *p < 0.05. Analysis of 4 independent experiments.

(E) Lysates were separated by gel electrophoresis before immunoblotting for GAPDH and FLAG to detect expression of the viral gene.

expressed protein through FLAG probe by immunoblot (Figure 2C). Compared to mock-infected cells, adenovirus infection resulted in a small but significant increase in total but not surface MR1, in an MOI-dependent manner. As a consequence, all statistical analysis of the modulation of MR1-GFP and surface MR1 and MHC-I by viral genes was calculated relative to the parental virus, with matching MOI, rather than mock-infected cells. Compared to cells infected with RAd-Ctrl (Figure 2B, dotted line) both ICP22 and US1.5 expression reduced total cellular MR1-GFP levels regardless of ligand treatment, although the reduction induced by US1.5 was significantly less than that induced by the full-length protein. The loss of cellular MR1 but not MHC-I was reconfirmed in the adenovirus-infected ARPE-19 MR1 cells which were lysed at 44 h p.i. and probed for MR1 and HLA-ABC by western blot (Figure 2C).

Reductions in surface MR1 replicated those of cellular MR1 suggesting that depleted levels of intracellular MR1 may be responsible for the loss of surface expression. Interestingly, although transfection of 293T cells with the ICP22-expressing plasmid resulted in increased surface MHC-I (Figure 2A), there was no significant difference in surface expression resulting from either ICP22 or US1.5 via adenovirus expression, nor was there any reduction in protein detected by western blot (Figure 2C).

Given that HSV-1 ICP22 downregulated expression of MR1 from both endogenous and foreign (murine stem cell virus LTR) promoters, but did not similarly affect endogenously expressed MHC-I, it was hypothesized that the viral genes specifically impacted MR1 protein rather than any MR1-specific or global impact on transcripts. Although MR1 antigen presentation is proteasome independent,[68] the substantial portion of MR1 that accumulates in the ER is likely degraded through proteasomal ER-associated degradation pathways.[51] We previously reported that HSV-1 targets immature MR1 for proteasomal degradation, by some unknown viral agent.[37] Indeed, treating the adenovirus-infected ARPE-19 MR1-GFP cells for 16 h with proteasomal inhibitor MG132 (5 μM) demonstrated a significant rescue of MR1-GFP compared to vehicle control (Figure 2D), which was not explained by any reduction in ICP22 or US1.5 protein expression (Figure 2E). This rescue was not observed with lysosomal inhibitor folimycin (50 nM).

Together these data demonstrate HSV-1 viral ICP22 (US1) and, to a lesser extent, the short form US1.5 promote proteasomal degradation of MR1, impacting its ability to respond to ligand availability and traffic to the plasma membrane. This downregulation is specific to MR1 and not applicable to classical antigen presentation MHC-I molecules.

vhs contributes to the loss of cellular MR1

Although ectopic ICP22 and US1.5 expression resulted in a significant loss of MR1-GFP, it is possible that other viral proteins contribute to the profound downregulation of cellular MR1 evident during HSV-1 infection.[37] The HSV-1 UL41 gene encodes a viral mRNA-specific endoribonuclease called virion host shutoff protein (vhs) that degrades predominantly cellular transcripts[69–71] through association with members of the cap binding complex including the RNA helicase accessory factor eIF4H.[72,73] Inhibition of cellular protein synthesis occurs immediately post infection with the release of vhs from infecting viral particles, followed by a second stronger wave of transcript degradation with the *de novo* expression of the late expression UL41 gene.[52]

To evaluate the impact of vhs expression on MR1, HSV-1 strain F UL41 gene was cloned into the pAdZ5-C5 adenovirus vector (RAd-vhs) and ARPE-19 MR1-GFP cells were infected as described. As detected by flow cytometry, cellular MR1 was strongly downregulated by 44 h p.i. regardless of ligand treatment (Figure 3A). Surface MR1 was also suppressed, with ligand treatment failing to promote strong surface expression, presumably due to the substantial depletion of cellular MR1. By contrast, endogenous surface MHC-I was only weakly downregulated by vhs expression. MR1 was not detectable by western blot from RAd-vhs-infected ARPE-19 MR1 cells at 44 h p.i. (Figure 3B). Despite the modest loss of surface MHC-I detected by flow cytometry (Figure 3A), a strong loss of cellular MHC-I proteins was evident (Figure 3B).

MR1 transcripts are downregulated during HSV-1 infection

Through alternative splicing the MR1 gene encodes four different protein isoforms.[74] The dominant and best characterized isoform encoded by the MR1A splice variant is responsible for activation of MAIT cells. The shorter MR1B protein lacks the α3 extracellular domain and accumulates in the ER as a homodimer rather than binding to β2m.[75] There is conflicting evidence as to whether MR1B traffics to the plasma membrane to activate MAIT cells or whether it plays a regulatory role by binding and retaining antigen in the ER.[75,76] The function of a soluble form lacking the transmembrane domain (MR1C) and another lacking the α3 domain but encoding a long 3′ untranslated sequence (MR1D) remains completely uncharacterized. Given that ectopic expression of vhs resulted in a strong downregulation of overexpressed MR1 protein, the relative amounts of endogenous and overexpressed transcripts were examined in human fibroblasts (HFs) and ARPE-19 MR1 cells infected with HSV-1 strain F at 2, 6, and 16 h p.i. Primers complementary to α1 and α2 regions were employed to detect total transcripts for MR1A, MR1B, and MR1C isoforms (MR1). Total MR1 transcripts were significantly reduced in infected HF cells by 6 h p.i. with further loss at the later time point (Figure 4A). In the ARPE-19 MR1 cells, where endogenous MR1 transcripts are likely outnumbered by the overexpressed MR1A isoform, this loss was detected at the 2 h time point and further reduced as the infection progressed (Figure 4B).

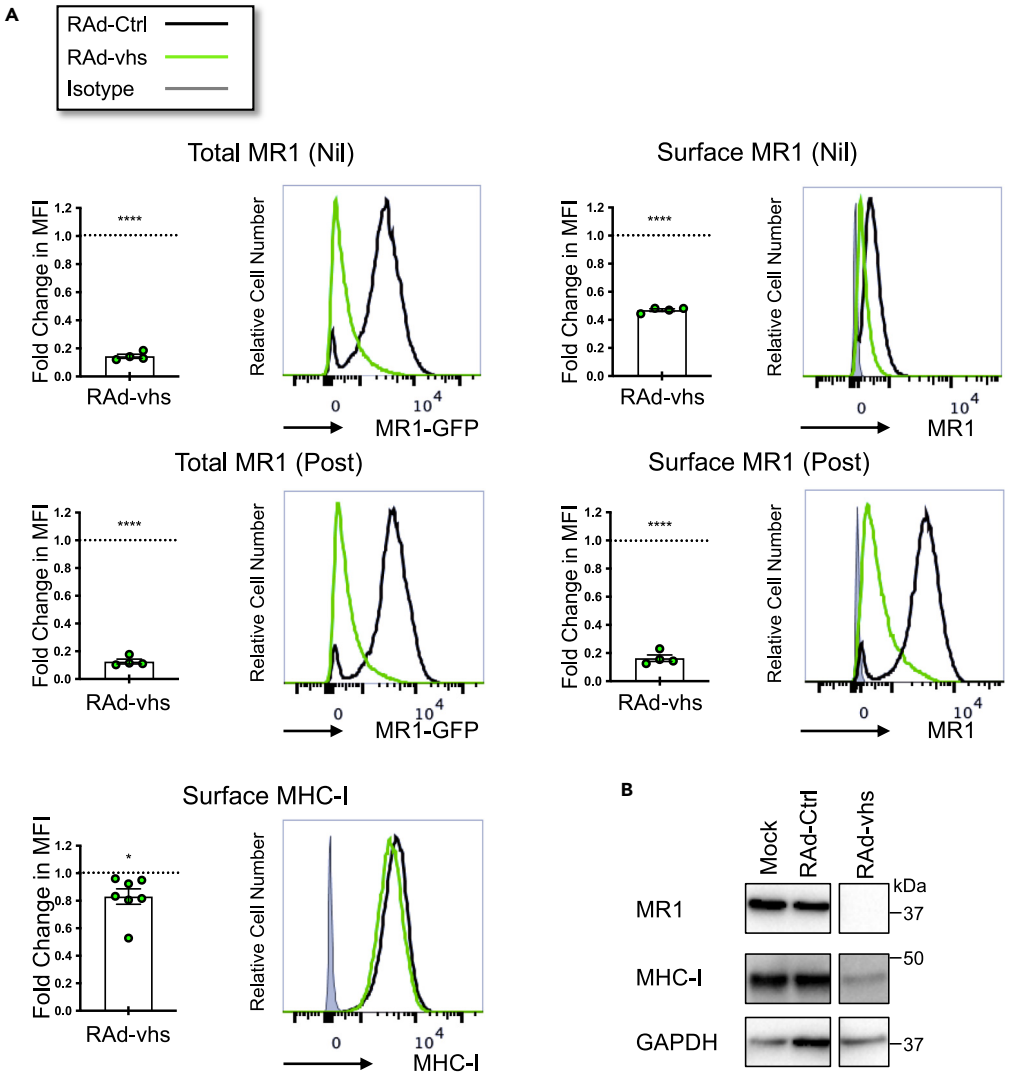

Figure 3. HSV-1 vhs protein expression modulates loss of total and surface MR1

(A) ARPE-19 MR1-GFP cells were infected with RAd-Ctrl adenovirus (black or dotted line) or RAd-Ctrl modified to encode HSV-1 vhs (RAd-vhs, green), MOI 100. Cells were left untreated (nil) or treated with Ac-6-FP (5 μM) for 4 h prior to harvesting at 44 h p.i. (post). Cells were stained for surface MR1, MHC-I, or matching isotype control (gray) and analyzed by flow cytometry. Fold change in MFI of live infected cells relative to RAd-Ctrl with matching ligand treatment is represented as mean ± SEM. Statistical significance was calculated by paired Student's *t* test, *p < 0.05, ****p < 0.0001. Analysis of 4 independent experiments.

(B) ARPE-19 MR1 cells were infected with RAd-Ctrl adenovirus or RAd-vhs or mock infected. Cells were harvested at 44 h p.i. and lysates were separated by gel electrophoresis before immunoblotting for MR1, MHC-I, and GAPDH.

While vhs plays a key role in modulation of the host transcriptome, other viral proteins contribute to this phenotype including ICP4, ICP27, and ICP22.[77,78] To determine whether virus lacking vhs expression rescued the loss of MR1 transcripts, HF cells were infected for 6 h with HSV-1 17syn$^+$ strain or the corresponding vhs deletion mutant 17(41-).[79] Two additional primers positioned at splice sites to specifically detect the MR1A and MR1B isoforms[76] were used to evaluate whether one isoform was preferentially targeted. There was a significant downregulation of the MR1A isoform and the combined isoforms from the intact parental virus, and, although there was a similar loss of MR1B, it was not statistically significant (p = 0.0753) (Figure 4C). Infection with the vhs mutant virus resulted in recovery of MR1A, MR1B, and total MR1 transcripts, with no significant difference to mock-infected cells. Again, although the trend was evident, the difference in MR1A isoforms between the parent and mutant virus was not statistically significant.

HSV-1 vhs mutant partially recovers loss of total MR1-GFP during early infection

At a late time point of infection the HSV-1 vhs deletion mutant does not rescue the loss of MR1;[37] however, here we show that the vhs-mediated loss of MR1 transcripts is rescued at early time points with the 17(41-) mutant virus. Furthermore, the contribution of US1 gene products to

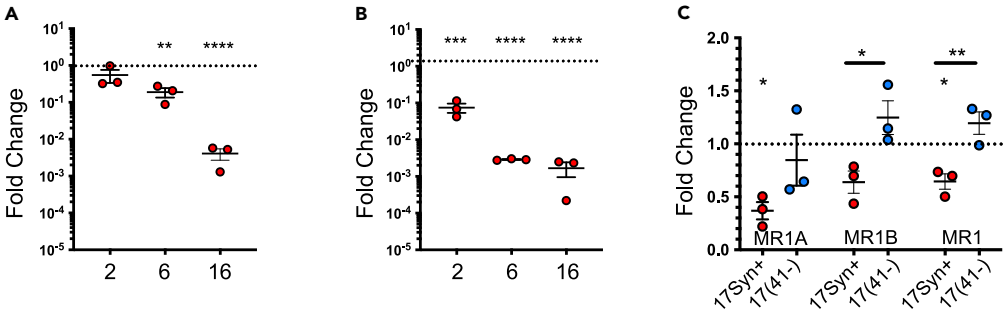

Figure 4. HSV-1 infection downregulates MR1 transcripts

(A) HF and (B) ARPE-19 MR1 cells were mock or HSV-1 strain F infected in parallel (MOI 5). Cell lysates were harvested at 2, 6, or 16 h p.i., and mRNA levels for MR1 and 18s were evaluated by RT-qPCR.

(C) HF cells were infected with HSV-1 strains 17syn+ (red) or 17(41-) lacking expression of vhs (blue) or mock infected in parallel. Cells were harvested at 6 h p.i. and mRNA levels or MR1A, MR1B, combined MR1 isoforms, and 18s were evaluated by RT-qPCR.

(A–C) Fold change compared to mock infection was calculated after normalizing to levels of 18s and is represented as mean ± SEM. Statistical significance to mock (dotted line) for MR1 was calculated by paired Student's *t* test *p < 0.05, **p < 0.005, ***p < 0.0005, ****p < 0.0001. Analysis of 3 independent experiments.

the loss of cellular MR1 confirms that more than one viral product contributes to the early loss of MR1 protein. To test whether the early loss of mRNA is reflected in a corresponding reduction in MR1 protein, ARPE-19 MR1-GFP cells were infected with HSV-1 17syn$^+$ and 17(41-) strains, optionally treated with MR1 ligand at 3 h p.i., and then harvested 3 h later. Regardless of ligand treatment there was a reduction in MR1-GFP at this early time point, which was partially rescued in cells infected with the vhs mutant (Figure 5B). In parallel, ARPE-19 cells were similarly infected and stained for the late HSV-1 glycoprotein gD. Expression of the viral glycoprotein gD was slightly higher in cells infected with the 17(41-) mutant compared to the parental 17syn+ strain (Figure 5A). This confirmed that delayed expression kinetics in the 17(41-) mutant were not responsible for the partial rescue of MR1-GFP.

In conclusion, vhs expression is sufficient to downregulate endogenous and overexpressed MR1, inhibiting the cell's ability to present MR1 ligand on the plasma membrane. This phenotype is driven by an early loss of MR1 isoform transcripts. Despite the substantial loss of transcripts by late time points, viral infection lacking vhs expression only partially rescues the loss of MR1 protein at early but not late times post infection, confirming that multiple viral products contribute to the modulation of MR1.

ICP22 and vhs expression downregulates MR1 in key subcellular compartments

As previously described, MR1 is predominantly ER associated, with ligand availability triggering maturation and egress through the secretory pathway. Once on the plasma membrane MR1 endocytoses and is predominantly degraded rather than recycled back to the surface membranes.[51,80] To further examine the effect of ICP22 and vhs on the loss of MR1 within cells, the relative amount of MR1 in subcellular compartments in the secretory and endocytic pathways of adenovirus RAd-ICP22- and RAd-vhs-infected ARPE-19 MR1-GFP cells was evaluated by high-throughput fluorescence microscopy. Cells were treated with ligand at the time of infection to promote MR1 maturation and trafficking and then stained for the nucleus (DAPI), ER (calreticulin), Golgi apparatus (GA, GM130), plasma membrane (wheat germ agglutinin), early endosomes (EEA1), or late endosomes/lysosomes (LAMP1) at 30 h p.i.[51,81] Expression of both viral proteins resulted in an overall reduction of MR1 within cells, compared to that detected in the RAd-Ctrl control infected samples (Figure 6A). The pattern of staining of subcellular compartments was unaffected by ICP22 and vhs expression compared to RAd-Ctrl (Figure 6B). Ilastik machine learning software[82] was trained to create a segmentation mask based on the subcellular markers so that the median MR1-GFP signal in each field of view (FOV) could be compared to the RAd-Ctrl infected samples for a quantitative analysis. A significant reduction in MR1 was detected in the immature pool in the ER, the secretory pathway (GM130), the plasma membrane, the endocytic (EEA1), and degradation pathways (LAMP1) (Figures 6C and 6E). The fold change of MR1-GFP intensity was calculated for each subcellular compartment with respect to the median for the FOV to establish whether all locations within the cell were equally depleted of MR1 protein (Figures 6D and 6F). The pool of ER-resident MR1 was preferentially lost, although the relative reduction was modest. Levels of MR1 in the GA were consistent with the median, while the plasma membrane and late endosomes/lysosomes were slightly increased. Surprisingly there was a stronger relative reduction of MR1 in the early endosomes, although the reason why these vesicles would be particularly depleted is unclear. Other than this compartment, the relatively uniform reduction in MR1 within the cell is consistent with loss emanating from a reduction of MR1 in the ER available to bind and traffic ligand to the plasma membrane.

HSV-2 modulation of MR1 mirrors HSV-1

Herpes simplex virus type 2 is thought to have emerged by cross-species transmission around 1.6 million years ago.[83] Parallel evolutionary pressures from the shared host combined with low rates of nucleotide substitution[83–85] have minimized the extent of divergence in viral products between HSV-1 and HSV-2. Given that the third, less closely related alphaherpesvirus VZV also modulates MR1,[38] the ability of HSV-2 to

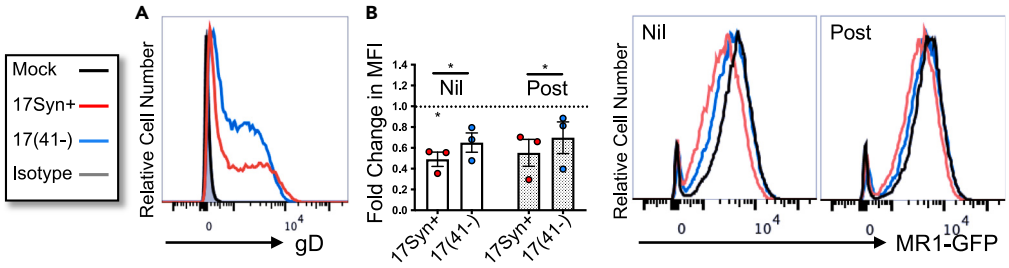

Figure 5. HSV-1 vhs deletion mutant partially recovers loss of total MR1-GFP

(A) ARPE-19 cells were mock (black), HSV-1 strains 17syn+ (red), or 17(41-) (blue) infected in parallel (MOI 3). Cells were harvested at 6 h p.i. and stained for late viral glycoprotein gD or matching isotype control (gray) and analyzed by flow cytometry. Histograms representative of two independent experiments.

(B) ARPE-19 MR1-GFP cells were mock (black), HSV-1 strains 17syn+ (red), or 17(41-) (blue) infected in parallel. Cells were left untreated (nil) or treated with Ac-6-FP (5 μM) at 3 h p.i. (post) before harvesting at 6 h p.i. Total MR1 (GFP) was detected by flow cytometry. Fold change in MFI of infected cells relative to mock-infected cells with matching ligand treatment is represented as mean ± SEM. Statistical significance was calculated by paired Student's *t* test *p < 0.05. Analysis of 3 independent experiments.

modulate MR1 was examined. To that end ARPE-19 MR1-GFP cells were infected with HSV-2 strain 186 (MOI 3), optionally treated with MR1 ligand 24 h before infection (Pre), 14 h post infection (Post), or left untreated (Nil) and then stained for surface MR1 at 18 h p.i. (Figure 7A). Total and surface MR1 were significantly downregulated in the absence of ligand and when cells were ligand treated post infection. While significant loss of total MR1 was also evident when cells were pre-treated with ligand, surface MR1 was comparable to mock-infected cells, reflecting a protection of pre-existing surface molecules from viral modulation also observed in MR1-GFP surface expression during HSV-1 infection.[37] Interestingly, while HSV-2-infected ARPE-19 cells expressing the wild-type MR1 molecule were similarly depleted of surface MR1 both in the absence of ligand and with post-infection treatment, surface MR1 was significantly upregulated with pre-infection ligand treatment (Figure 7B). This was also observed with HSV-1 infection[37] suggesting the GFP tag may block the upregulation of surface MR1 molecules during both HSV-1 and HSV-2 infection.

The one site of immature N-linked glycosylation on the MR1 α1 extracellular domain is remodeled into the mature form when the protein leaves the ER and traffics through the secretory pathway. Digest of the MR1 protein by endoglycosidase H (Endo H) reduces the molecular weight of immature but not the mature glycosylated form resulting in the detection of two separate MR1 bands by western blot. ARPE-19 MR1 cells were infected with HSV-2 and treated with one of the three ligand conditions as described earlier. Cell lysates were then digested with Endo H and probed for MR1, GAPDH (cellular control), and ICP27 (viral control).

No MR1 was detected in the HSV-2-infected samples lacking ligand or treated at 14 h p.i., consistent with the loss of both total and surface MR1 detected by flow cytometry under the same assay conditions (Figure 7C). Only a faint band of Endo H-resistant, mature MR1 (black arrow) remained in the infected cells pre-treated with ligand, at a comparable strength to the uninfected samples, indicating that only the mature, pre-existing MR1 is protected from downregulation by HSV-2.

To examine the impact of HSV-2 on MR1 mRNA HF cells were infected for 6 h and the transcripts amplified by RT-qPCR using the MR1A, MR1B, and pan-specific MR1 primers. A significant reduction in transcripts was detected using all three primer sets indicating that during HSV-2 infection loss of MR1 transcripts contributes to the reduction in MR1 protein (Figure 7D). Together these data demonstrate that HSV-2 infection mirrors the HSV-1-induced MR1 phenotype characterized by the early loss of MR1A, B, total MR1 transcripts, and near complete loss of immature MR1 protein with only mature and surface MR1 protected from HSV-2 downregulation.

Relative retention of MR1 on plasma membrane during HSV-1 and HSV-2 infection

Although the loss of MR1 in HSV-1- and HSV-2-infected epithelial cells is pronounced, it is not uniformly lost within the cell, given the retention of mature Endo H-resistant forms (Figure 6B).[37] To further examine the effect of infection on the loss of MR1 within the subcellular compartments in the secretory and endocytic pathways, HSV-1- and HSV-2 (MOI 5)-infected ARPE-19 MR1-GFP cells were stained and examined by fluorescence microscopy at 6 h p.i. as previously described. Given that there was no detectable modulation of surface MR1 by flow cytometry (Figures 5 and 7), the MOI was increased to 5 to promote a more rapid transition through the viral expression cascade. Cells were pre-treated with ligand for 16 h prior to infection to promote MR1 maturation and trafficking. The contribution of vhs to the loss of MR1 was explored by comparing the HSV-1 17(41-) vhs mutant to the parental strain 17syn+.

The staining of subcellular compartments in the infected cells was qualitatively consistent with mock-infected cells (Figure S1), lacking the marked rearrangement of cellular markers and cytoplasmic effect that is characteristic of later stages of infection.[86] Within the FOV cell mask MR1 was significantly downregulated in HSV-2 and HSV-1 cells, with the loss partially recovered in the absence of vhs expression (Figures 8A and 8C). There was an absolute loss of MR1 in each subcellular compartment, although the loss from the plasma membrane associated with HSV-2 infection was modest and the vhs mutant similarly had limited impact on EEA1-associated MR1. Furthermore, there was a partial recovery associated with the vhs mutant in all compartments other than the plasma membrane, where the downregulation was consistent between parental strain and vhs mutant.

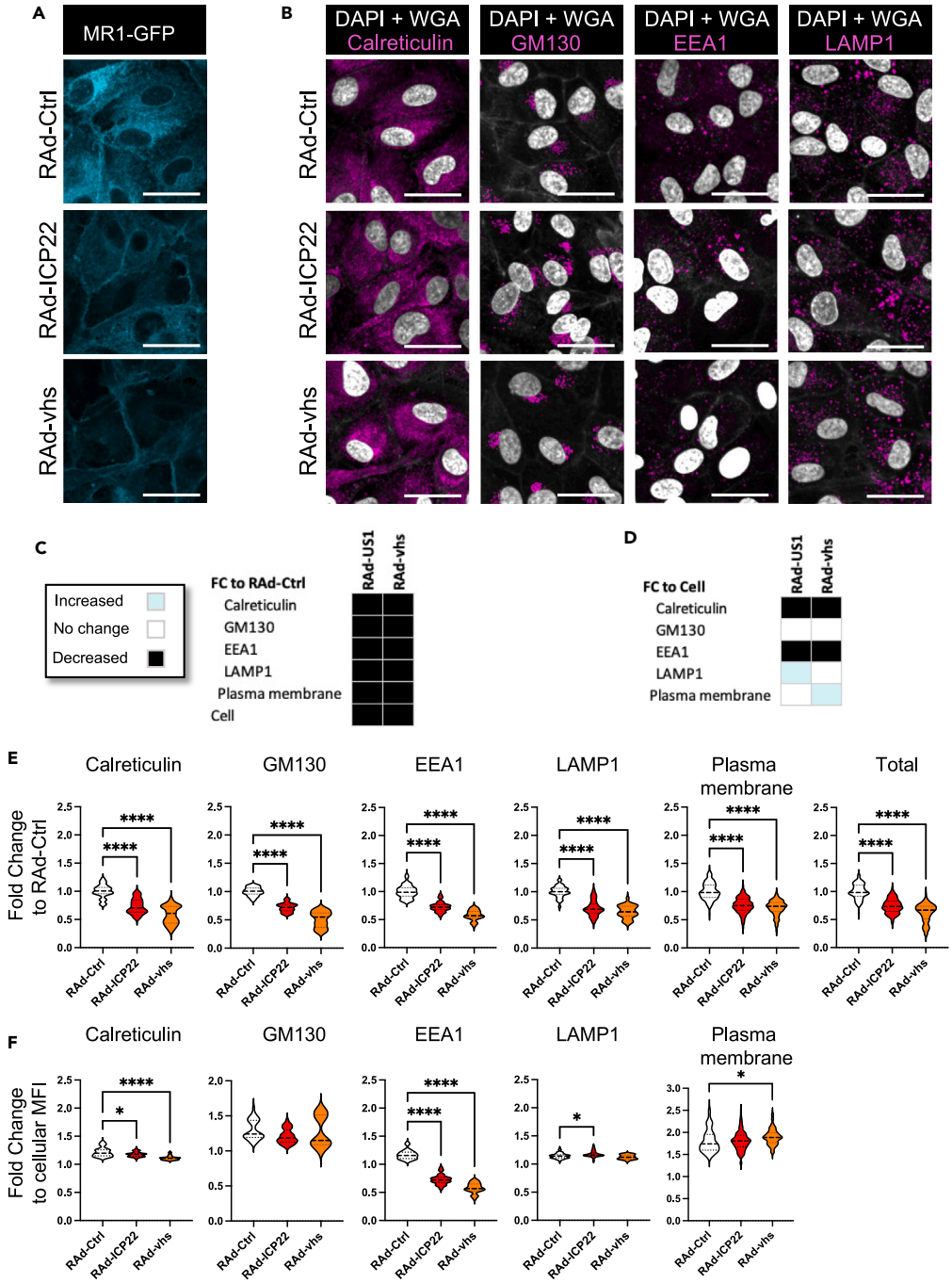

Figure 6. ICP22 and vhs expression downregulates MR1 in key subcellular compartments

ARPE-19 MR1-GFP cells were infected with RAd-Ctrl adenovirus (white) or RAd-Ctrl modified to encode HSV-1 ICP22 (RAd-ICP22, red) or HSV-1 vhs (RAd-vhs, orange), MOI 100. Cells were treated with Ac-6-FP (5 μM) at time of infection. Cells were stained at 30 h p.i. with wheat germ agglutinin (WGA) (plasma membrane) and then permeabilized and stained for calreticulin (ER), GM130 (Golgi apparatus), EEA1 (early endosomes) or LAMP1 (late endosomes/lysosomes), and DAPI (nucleus).

(A–F) (A) Representative images of MR1-GFP and (B) images of DAPI and WGA (white) merged with calreticulin, GM130, EEA1, or LAMP1 (magenta) from two independent experiments. Scale bar 50 μm. Cell segmentation completed with ilastik software and quantification of fold change of MR1 intensity relative to RAd-Ctrl (C and E) or total cellular MR1 within each field of view (FOV) (D and F) performed with ImageJ software. Violin plots of individual fold change points are depicted with median + quartiles. Statistical significance was calculated with one-way ANOVA, *$p < 0.05$, ****$p < 0.0001$. Analysis of at least 14 FOV in two independent experiments.

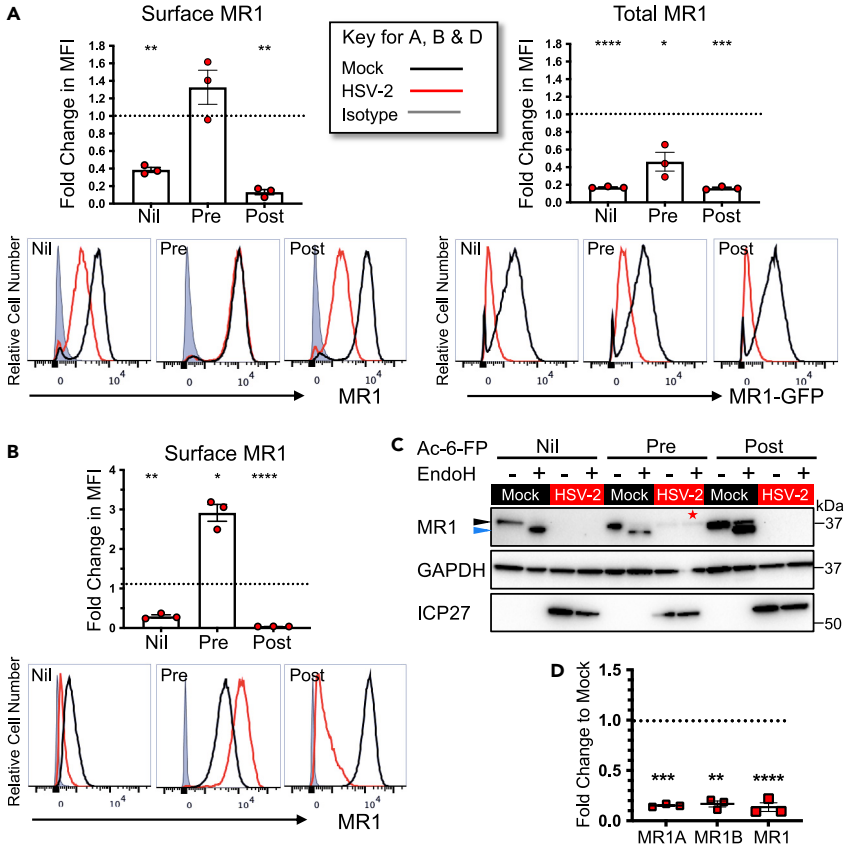

Figure 7. HSV-2 targets immature MR1 protein while ligand-bound mature MR1 is protected

(A) ARPE-19 MR1-GFP or (B and C) ARPE-19 MR1 cells were mock or HSV-2 infected in parallel (MOI 3). Cells were either left untreated (Nil) or treated with Ac-6-FP (5 μM) for 24 h prior to infection (Pre) or at 14 h p.i. (Post) before harvesting at 18 h p.i.

(A and B) Cells were stained for surface MR1 or isotype control (gray) and analyzed by flow cytometry. Fold change in MFI of infected cells (red) relative to mock-infected cells (black) with matching ligand treatment is represented as mean ± SEM. Statistical significance was calculated by paired Student's *t* test *$p < 0.05$, **$p < 0.005$, ***$p < 0.0005$, ****$p < 0.0001$.

(C) Cell lysates were left undigested or EndoH digested before immunoblotting for MR1, GAPDH, GFP, or ICP27. Endo H-resistant MR1 is denoted with black triangle while Endo H susceptible bands denoted with blue triangle. Red star denotes retained EndoH-resistant band in HSV-2-infected cells pre-treated with ligand.

(D) HF cells were infected with HSV-2 or mock infected in parallel. Cells were harvested at 6 h p.i. and mRNA levels of MR1A, MR1B, combined MR1 isoforms, and 18s were evaluated by RT-qPCR. Fold change compared to mock infection was calculated after normalizing to levels of 18s, represented as mean ± SEM. Statistical significance to mock (dotted line) for MR1 was calculated by paired Student's *t* test **$p < 0.005$, ***$p < 0.0005$, ****$p < 0.0001$. Analysis of 1 (C) or 3 (A, B, D) independent experiments.

The relative amount of MR1-GFP within each subcellular compartment with respect to the median for the FOV was also calculated and then expressed as a fold change to the proportion detected in the control infected cells (Figures 8B and 8D). MR1 in the ER, GA, and late endosomes/lysosomes was more strongly depleted compared to the median within the FOV, with the vhs mutant mediating a relative recovery of MR1 only in late endosomes. By contrast, MR1 on the plasma membrane was instead retained (HSV-2, 17(41-)) or upregulated (HSV-1 17syn+). Similarly there was no relative reduction in the EEA1-labeled compartments (Figure 8E) associated with HSV-1, HSV-1 17syn+, or 17(41-) viral infections.

While there is some consistency at this early time point post infection with the absolute and relative reduction of MR1 within cellular compartments resulting from the expression of ICP22 and vhs, there are also some interesting differences. Both models drive a relatively stronger loss of MR1 from the ER, even when the virus lacks vhs expression. However, viral infection, including from the vhs mutant, results in a similarly stronger relative loss of MR1 from the GA which was not evident with ectopic ICP22 or vhs protein expression. Furthermore viral infection failed to preferentially target loss of MR1 from early endosomes, with some of the punctate cytoplasmic accumulations colocating with EEA1. Consistent with the finding that vhs expression preferentially targeted the EEA1-associated MR1, there was a significant recovery in the absolute amount of MR1 with the vhs mutant. Together these results indicate that during the initial hours post infection MR1 is preferentially lost from the ER pool and secretory and degradation pathways, but other mechanism(s) may impact the amount of MR1 on the plasma membrane and in early endocytic compartments.

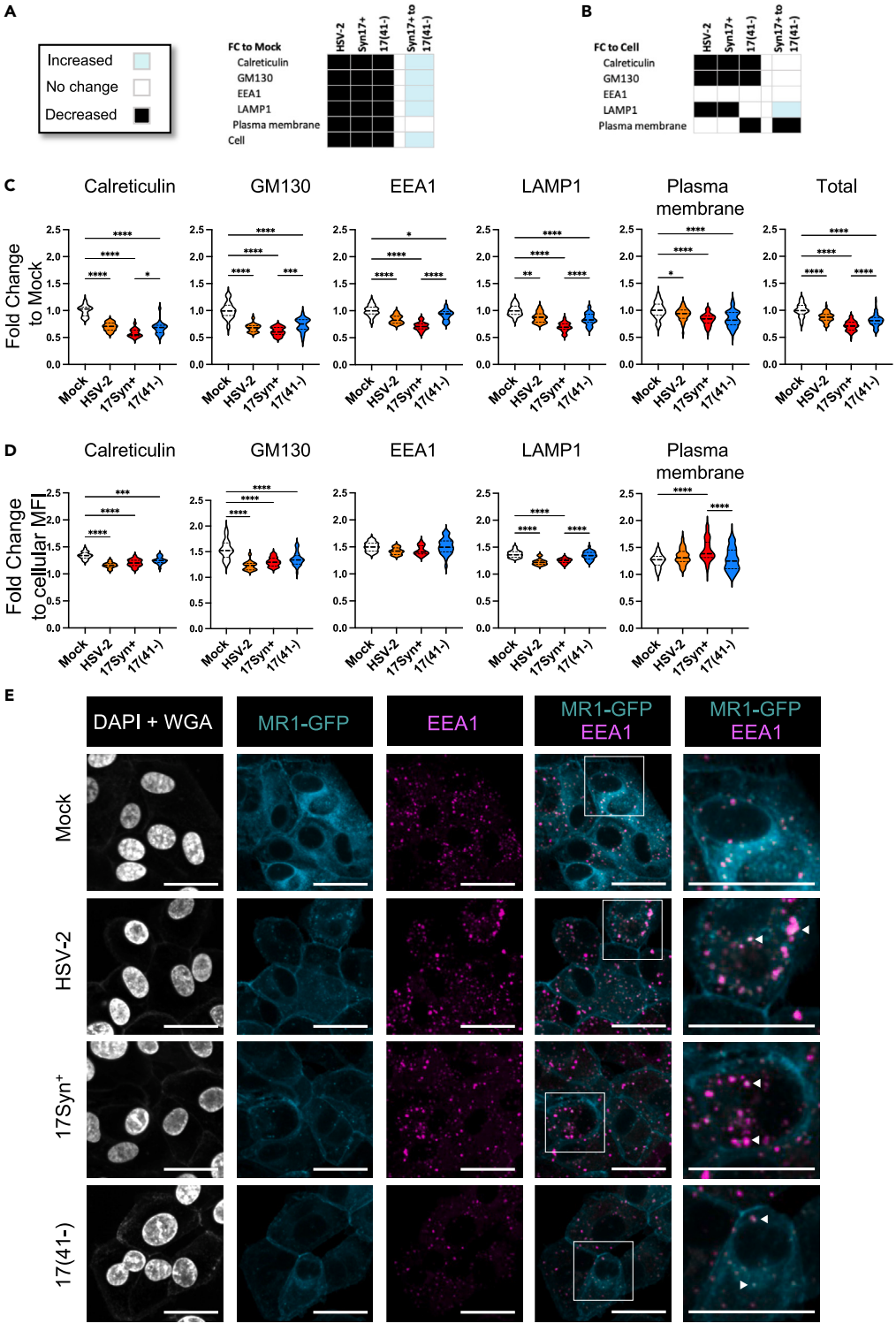

Figure 8. HSV-1- and HSV-2-mediated loss of MR1 is strongest in the ER and secretory pathway and is partially recovered in absence of vhs expression

(A–D) ARPE-19 MR1-GFP cells were infected (MOI 5) with HSV-2 (orange), HSV-1 strains 17syn+ (red), or 17(41-) lacking expression of vhs (blue) or mock (white) infected in parallel. Cells were treated with Ac-6-FP (5 μM) for 16 h prior to infection. Cells were stained at 6 h p.i. with wheat germ agglutinin (WGA) (plasma membrane) and then permeabilized and stained for calreticulin (ER), GM130 (Golgi apparatus), EEA1 (early endosomes) or LAMP1 (Late endosomes/lysosomes), and DAPI (nucleus). Cell segmentation completed with ilastik software and quantification of fold change (FC) in MR1 intensity relative to mock (A and C) or total cellular MR1 within each field of view (FOV) (B and D) performed with ImageJ software. Violin plots of individual fold change points are

Figure 8. *Continued*

depicted with median + quartiles. Statistical significance was calculated with one-way ANOVA, *p < 0.05, **p < 0.005, ***p < 0.0005, ****p < 0.0001. Analysis of at least 14 FOV in two independent experiments.

(E) Representative images of DAPI + WGA, MR1-GFP, EEA1, and merged images with white arrows highlighting examples of colocation in enlarged image (box) on right. Scale bar 50 μm.

DISCUSSION

This study identifies several herpes simplex virus gene products that modulate MR1 expression, specifically the IE proteins ICP22 and US1.5 and the viral RNase vhs. It also establishes impacts on MR1 transcription by vhs, and protein degradation mediated by ICP22, and to a lesser extent the shorter gene product US1.5. Finally it demonstrates that an additional alphaherpesvirus, HSV-2, also targets MR1 expression. Although the impact of the multifaceted modulation of this key resident immune cell population is not explicitly examined, delayed and diminished MAIT cell effector capacity is likely to impact viral clearance and MAIT cell cytolytic killing of virally infected cells, thus promoting more efficient establishment of viral latency and transmission to a new host.

Cellular MR1 is progressively reduced during the first 6 h of infection[37] placing IE gene products high on the list of candidates. Infection with a virus lacking expression of the IE protein ICP0, an E3 ubiquitin ligase responsible for degradation of various cellular proteins,[42,87–89] failed to rescue the phenotype.[37] A second candidate ICP47, responsible for blocking peptide loading into the antigen cleft of MHC-I molecules, was initially dismissed, given that early studies found that MR1 could present antigen independent of TAP, the member of the PLC that controls import of the peptides into the ER lumen.[90,91] Furthermore, ectopic expression of ICP47 in human dendritic cells and lung epithelial cells fails to inhibit interferon-γ secretion by MR1-restricted T cell clones in response to mycobacteria tuberculosis challenge.[92] However, a more recent study revealed that MR1 is stabilized in the ER by the PLC,[47] warranting examination of the effect of ICP47 binding. HSV-1 infection of epithelial cells overexpressing MR1-GFP with a virus lacking ICP47 expression however failed to rescue the loss of total or surface MR1 at either early or late time points (Figure 1) demonstrating that this viral protein modulates MHC-I but not MR1 antigen presentation.

A third IE protein ICP22, encoded by the US1 gene, was screened due to its multifaceted control of cellular and viral transcription, involvement in protein quality control,[57] and the demonstrated capacity of the HSV-2 homolog to act as an E3 ubiquitin ligase.[64] Although ICP22 is predominantly nuclear in location,[93] ICP22 expression reduces the aggregation of non-native proteins in the cytoplasm, confirming that its localization is not restricted to the nucleus.[57] Ectopic plasmid expression of HSV-1 ICP22 resulted in a downregulation of endogenous surface MR1. While the full-length protein induced a strong reduction in MR1, the shorter US1.5 protein demonstrated a more limited loss based on the MR1-GFP signal detected by flow cytometry, although there was substantial loss of MR1 resulting from expression of both constructs detected by immunoblot (Figure 2). Inhibition of proteasomal and lysosomal protein degradation established that US1 gene products promote proteasomal degradation of MR1, consistent with the loss of MR1 from the ER, GA, plasma membrane, and early and late endocytic compartments with ectopic ICP22 expression (Figure 6). This significant finding explains the MG132-mediated rescue of MR1 protein during HSV-1 infection[37] and represents an additional immunomodulatory function of the US1 gene.

The differential strength of the modulation between ICP22 and US1.5 suggests that the N-terminal domain may be required for optimal modulation of MR1. Interestingly, the N-terminal domain is proposed as the site of Hsc70 interaction associated with protein quality control functionality.[57] However, a definitive understanding of the functional overlap between ICP22 and US1.5 is complicated by the lack of agreement over whether US1.5 translation commences from residues 90, 157,[58,65] or 171 as was used in this study.[60,66]

ICP22 acts as a *trans* regulator to promote late viral gene expression; consequently ICP22 null mutants demonstrate attenuated viral replication, impaired expression of vhs (Ng et al., 1997), and progeny containing reduced amounts of some glycoproteins.[94–96] This complicates evaluating the contribution of US1 gene products to MR1 modulation through infection with an US1 null virus.

Although this study demonstrates that ectopic expression of both ICP22 and US1.5 is sufficient to downregulate MR1 expression, future studies are required to identify how ICP22 promotes MR1 proteasomal degradation, evaluate the HSV-2 homologs, and confirm the contribution of ICP22 and US1.5 to the loss of MR1 in the context of viral infection.

HSV-1 and HSV-2 both encode homologs of the potent viral RNase vhs that contribute to pathogenesis.[97–100] Vhs effectively suppresses multiple arms of the innate and antiviral response including blocking detection of viral DNA,[101] interferon signaling pathways,[102] interferon stimulated gene expression,[103–105] and inactivation of dendritic cells.[106] In this study we extend the list of antigen presentation molecules downregulated by vhs from MHC-I and MHC-II[107,108] to also include MR1. Interestingly UV-inactivated HSV-1 effects a modest but significant reduction in surface MR1 which could be derived from vhs released from the tegument of infecting viral particles.[37] HSV-1 vhs expressed from an adenovirus construct effected a reduction in cellular MR1-GFP in ARPE-19 cells and consequently failed to upregulate surface MR1 in response to ligand treatment. Consistent with this result, MR1 was lost from all 5 of the subcellular locations examined from fluorescent microscopy (Figure 6), reflecting loss of MR1 emanating from the earliest stage in the MR1 biosynthesis pathway.

Four different protein isoforms are synthesized from the *mr1* gene through differential splicing.[74] While the MR1A isoform is relatively well characterized as the membrane-bound form that presents ligands to MAIT cells, there is evidence suggesting the MR1B isoform may prevent MAIT cell response to non-pathogenic levels of riboflavin biosynthesis through ligand binding to MR1B homodimers retained in the ER.[75,76] Using primers designed to detect MR1A, B, and total transcripts the levels of endogenous and MR1A-overexpressed transcripts were examined at three time points following infection (Figure 4). HSV-1 infection resulted in a downregulation of overexpressed and endogenous MR1 transcripts by 2 and 6 h p.i., respectively. Using MR1A- and MR1B-specific primers it was confirmed that in HF cells endogenous levels of both were depleted by 6 h p.i., but that infection with the vhs 17(41-) deletion mutant rescued the loss of both isoforms and the combined MR1 transcripts to those of mock-infected cells.

Multiple HSV gene products have global impacts on transcripts, including vhs, ICP4, ICP22, and the ICP27-mediated disruption of transcription termination.[109] Unexpectedly, deletion of the short non-coding RNA sequence sncRNA1 from the HSV-1 genome drives increased MR1 transcript levels in the trigeminal ganglia of mice after ocular infection.[110] Currently, there is an extremely limited understanding of the factors affecting regulation of the ubiquitously expressed MR1 gene, although it has been shown to vary between cell types,[111] is upregulated by inflammatory cytokines associated with type 1 diabetes,[112] and the ratio of MR1A to MR1B isoforms varies between tissues and individuals.[76] One publication that has examined MR1 transcripts during viral infection detected elevated MR1 transcripts in hepatocytes infected with hepatitis B virus, with an associated increase in cytotoxicity of MAIT cells.[113] Although vhs facilitates the degradation of many host transcripts, infection of the ARPE-19 MR1-GFP cells with the vhs mutant 17(41-) demonstrated a complete rescue of MR1 transcripts (Figure 4C) and a partial rescue of the loss of total cellular MR1 protein at 6 h p.i. (Figure 5B). This suggests that vhs is the dominant mechanism of MR1-mediated loss of MR1 transcripts, and that this contributes to the modulation of MR1 antigen presentation during HSV-1 infection. A more thorough investigation of the effects of HSV-1 products on MR1 promoter activity and transcript longevity would be of additional interest.

Given that HSV-1, VZV, and HCMV all modulate MR1 antigen presentation,[37,38] HSV-2 was also examined and found to be capable of modulating MR1 in a ligand-dependent fashion that mirrored the HSV-1-induced phenotype. Furthermore, lower levels of MR1A, MR1B, and total MR1 transcripts were detected in HSV-2-infected cells (Figure 7D), potentially implicating HSV-2 vhs in the modulation of MR1. During HSV-1 infection of ARPE-19 MR1 cells, we have previously published immunoblots demonstrating that loss of MR1 progressively increases during the first 6 h post infection.[37] Any future study that examines the contribution of HSV-2 gene products to the modulation of the MR1, including the HSV-2 vhs ICP22 and US1.5 homologs, may benefit from such an examination.

Interestingly, both HSV-1 and HSV-2 infection promoted increased surface MR1 when cells were pre-treated with Ac-6-FP ligand; however, there was no significant difference in the abundance of the GFP-tagged molecule with either virus compared to mock-infected cells.[37] Recently it was shown that MR1 endocytosis occurs via AP2 recognition of its C-terminal cytoplasmic tail.[80] Interestingly, the C-terminal fusion of MR1 with GFP resulted in reduced endocytosis likely due to the GFP molecule preventing AP2 binding to the tail.[37] Therefore it is possible that the increased cell surface stability of MR1, but not MR1-GFP molecules, is due to HSV interrupting AP2-mediated endocytosis of MR1; however this remains to be investigated.

As previously discussed, expression of both HSV-1 ICP22 and vhs proteins resulted in a cell-wide reduction in MR1; however, manipulation of ligand timing during HSV-1[37] and HSV-2 infection revealed retention of some mature Endo H-resistant protein. To further examine the relative pattern of intracellular loss, ARPE-19 MR1-GFP cells were pre-treated with ligand to promote MR1-GFP distribution, infected with HSV-1 or HSV-2, and then examined by fluorescence microscopy at 6 h pi. Even at this early time point there was loss from the ER, GA, plasma membrane, and early and late endocytic compartments (Figure 8). Cells similarly infected with the HSV-1 vhs mutant virus demonstrated a partial restoration of MR1 from each compartment resulting from the recovery of transcripts. Unlike that observed with ectopic ICP22 and vhs expression, MR1 associated with EEA1-labeled compartments was downregulated at levels comparable to the whole cell. Furthermore, surface MR1 was relatively elevated compared to the median cellular MR1 in the HSV-1 17Syn+-infected cells suggesting that additional factors modulate localization of mature MR1 during viral infection.

In conclusion, these findings increase our understanding of the mechanisms employed by HSV-1 to protect against the targeted MR1-dependent attack by resident MAIT cells by establishing that during HSV-1 infection vhs targets MR1 transcripts while ICP22 targets MR1 for proteasomal degradation. In addition, we establish that HSV-2 also downregulates MR1, further implicating the MR1 antigen presentation pathway as a target conserved across multiple herpesviruses.

Limitations of the study

This study utilized GFP-tagged overexpressed MR1 to assess the modulation of MR1 protein in intracellular compartments during herpes simplex virus infection, and resulting from the ectopic expression of the HSV-1 US1 and UL41 viral gene products. Given that addition of the C-terminal GFP tag slightly delays MR1 endocytosis,[80] evaluation of the localization of untagged MR1 under the same experimental conditions would be of interest; however, comparisons would need to take into consideration that a pan-MR1 antibody capable of detecting all conformations of the MR1 is currently unavailable.

The loss of total MR1 by ectopic expression of ICP22 or US1.5 was rescued by treatment with proteasomal inhibitor MG132. Additional research is required to confirm whether these viral proteins promote proteasomal degradation of MR1 through direct interaction with MR1, or whether they encode ubiquitin ligase functionality.

The study did not examine vhs, ICP22, or US1.5 from HSV-2, so it is not possible to conclude that they modulate MR1 in line with that observed with their respective HSV-1 homologs. This requires independent investigation.

STAR★METHODS

Detailed methods are provided in the online version of this paper and include the following:

- KEY RESOURCES TABLE
- RESOURCE AVAILABILITY
  - Lead contact
  - Materials availability
  - Data and code availability

SUPPLEMENTAL INFORMATION

Supplemental information can be found online at https://doi.org/10.1016/j.isci.2024.108801.

ACKNOWLEDGMENTS

C.S. and T.V. were each supported by an Australian Postgraduate Award/Australian Government Research Training Program Scholarship. We acknowledge grant support from the National Health and Medical Research Council (NHMRC) of Australia, 198704 (A.A. and B.S.), 2003192 (H.E.G.M.), and 1113293 and 1154502 (J.A.V.), the US National Institutes of Health RO1 R01AI148407 (J.R. and J.A.V.), NHMRC Leadership Investigator grants 2008913 (J.R.) and 2016969 (J.A.V.), Australian Research Council (ARC) DP170102471 (J.A.V.), Wellcome Trust 204870/Z/16/Z (R.J.S.), and UK Medical Research Council (MRC) MR/S00971X/1 (R.J.S.).

The authors wish to thank members of the Herpesvirus Pathogenesis and Viral Immunology research groups (School of Medical Sciences, The University of Sydney) for helpful discussions and acknowledge the Sydney Cytometry Core Research Facility, a joint initiative of Centenary Institute and the University of Sydney, for assistance with flow and imaging cytometry experiments.

AUTHOR CONTRIBUTIONS

Conceptualization, C.S.; methodology, C.S., H.E.G., B.P.M., J.G.B.; formal analysis, C.S.; resources, T.V., D.C.T., J.R., R.S., J.A.V.; writing – original draft, C.S.; writing – review and editing, A.A., B.S.; funding acquisition, A.A., B.S. All authors have read and agreed to the published version of the manuscript.

DECLARATION OF INTERESTS

The authors declare no competing interests.

Received: March 16, 2023
Revised: September 18, 2023
Accepted: January 2, 2024
Published: January 4, 2024

REFERENCES

1. Dusseaux, M., Martin, E., Serriari, N., Péguillet, I., Premel, V., Louis, D., Milder, M., Le Bourhis, L., Soudais, C., Treiner, E., and Lantz, O. (2011). Human MAIT cells are xenobiotic-resistant, tissue-targeted, CD161(hi) IL-17-secreting T cells. Blood *117*, 1250–1259.
2. Gibbs, A., Leeansyah, E., Introini, A., Paquin-Proulx, D., Hasselrot, K., Andersson, E., Broliden, K., Sandberg, J.K., and Tjernlund, A. (2017). MAIT cells reside in the female genital mucosa and are biased towards IL-17 and IL-22 production in response to bacterial stimulation. Mucosal Immunol. *10*, 35–45.
3. Tang, X.Z., Jo, J., Tan, A.T., Sandalova, E., Chia, A., Tan, K.C., Lee, K.H., Gehring, A.J., De Libero, G., and Bertoletti, A. (2013). IL-7 Licenses Activation of Human Liver Intrasinusoidal Mucosal-Associated Invariant T Cells. J. Immunol. *190*, 3142–3152.
4. Constantinides, M.G., Linehan, J.L., Sen, S., Shaik, J., Roy, S., LeGrand, J.L., Bouladoux, N., Adams, E.J., and Belkaid, Y. (2017). Mucosal-associated invariant T cells respond to cutaneous microbiota. J. Immunol. *198*, 218.15.
5. Leeansyah, E., Svärd, J., Dias, J., Buggert, M., Nyström, J., Quigley, M.F., Moll, M., Sönnerborg, A., Nowak, P., and Sandberg, J.K. (2015). Arming of MAIT Cell Cytolytic Antimicrobial Activity Is Induced by IL-7 and Defective in HIV-1 Infection. PLoS Pathog. *11*, e1005072.
6. Porcelli, S., Yockey, C.E., Brenner, M.B., and Balk, S.P. (1993). Analysis of T-cell antigen receptor (TCR) expressiong by human peripheral blood CD4-8-alpha/beta T-cells demonstrates preferential use of several V-beta genes and an invariant TCR alpha-chain. J. Exp. Med. *178*, 1–16.
7. Tilloy, F., Treiner, E., Park, S.H., Garcia, C., Lemonnier, F., de la Salle, H., Bendelac, A., Bonneville, M., and Lantz, O. (1999). An invariant T cell receptor alpha chain defines a novel TAP-independent major histocompatibility complex class Ib-restricted alpha/beta T cell subpopulation in mammals. J. Exp. Med. *189*, 1907–1921.
8. Reantragoon, R., Corbett, A.J., Sakala, I.G., Gherardin, N.A., Furness, J.B., Chen, Z., Eckle, S.B.G., Uldrich, A.P., Birkinshaw, R.W., Patel, O., et al. (2013). Antigen-loaded MR1 tetramers define T cell receptor heterogeneity in mucosal-associated invariant T cells. J. Exp. Med. *210*, 2305–2320.
9. van Wilgenburg, B., Loh, L., Chen, Z., Pediongco, T.J., Wang, H., Shi, M., Zhao, Z., Koutsakos, M., Nüssing, S., Sant, S., et al. (2018). MAIT cells contribute to protection against lethal influenza infection in vivo. Nat. Commun. *9*, 4706.
10. Loh, L., Wang, Z., Sant, S., Koutsakos, M., Jegaskanda, S., Corbett, A.J., Liu, L.,

Fairlie, D.P., Crowe, J., Rossjohn, J., et al. (2016). Human mucosal-associated invariant T cells contribute to antiviral influenza immunity via IL-18-dependent activation. Proc. Natl. Acad. Sci. USA *113*, 10133–10138.

11. Kjer-Nielsen, L., Patel, O., Corbett, A.J., Le Nours, J., Meehan, B., Liu, L., Bhati, M., Chen, Z., Kostenko, L., Reantragoon, R., et al. (2012). MR1 presents microbial vitamin B metabolites to MAIT cells. Nature *491*, 717–723.
12. van Wilgenburg, B., Scherwitzl, I., Hutchinson, E.C., Leng, T., Kurioka, A., Kulicke, C., de Lara, C., Cole, S., Vasanawathana, S., Limpitikul, W., et al. (2016). MAIT cells are activated during human viral infections. Nat. Commun. *7*, 11653.
13. Phetsouphanh, C., Phalora, P., Hackstein, C.P., Thornhill, J., Munier, C.M.L., Meyerowitz, J., Murray, L., VanVuuren, C., Goedhals, D., Drexhage, L., et al. (2021). Human MAIT cells respond to and suppress HIV-1. Elife *10*.
14. Lal, K.G., Kim, D., Costanzo, M.C., Creegan, M., Leeansyah, E., Dias, J., Paquin-Proulx, D., Eller, L.A., Schuetz, A., Phuang-Ngern, Y., et al. (2020). Dynamic MAIT cell response with progressively enhanced innateness during acute HIV-1 infection. Nat. Commun. *11*, 272.
15. Paquin-Proulx, D., Greenspun, B.C., Costa, E.A.S., Segurado, A.C., Kallas, E.G., Nixon, D.F., and Leal, F.E. (2017). MAIT cells are reduced in frequency and functionally impaired in human T lymphotropic virus type 1 infection: Potential clinical implications. PLoS One *12*, e0175345.
16. Yong, Y.K., Saeidi, A., Tan, H.Y., Rosmawati, M., Enström, P.F., Batran, R.A., Vasuki, V., Chattopadhyay, I., Murugesan, A., Vignesh, R., et al. (2018). Hyper-Expression of PD-1 Is Associated with the Levels of Exhausted and Dysfunctional Phenotypes of Circulating CD161(++)TCR iV alpha 7.2(+) Mucosal-Associated Invariant T Cells in Chronic Hepatitis B Virus Infection. Front. Immunol. *9*, 472.
17. Yong, Y.K., Tan, H.Y., Saeidi, A., Rosmawati, M., Atiya, N., Ansari, A.W., Rajarajeswaran, J., Vadivelu, J., Velu, V., Larsson, M., and Shankar, E.M. (2017). Decrease of CD69 levels on TCR Vα7.2(+)CD4(+) innate-like lymphocytes is associated with impaired cytotoxic functions in chronic hepatitis B virus-infected patients. Innate Immun. *23*, 459–467.
18. Dias, J., Hengst, J., Parrot, T., Leeansyah, E., Lunemann, S., Malone, D.F.G., Hardtke, S., Strauss, O., Zimmer, C.L., Berglin, L., et al. (2019). Chronic hepatitis delta virus infection leads to functional impairment and severe loss of MAIT cells. J. Hepatol. *71*, 301–312.
19. Huang, W., He, W., Shi, X., Ye, Q., He, X., Dou, L., and Gao, Y. (2020). Mucosal-associated invariant T-cells are severely reduced and exhausted in humans with chronic HBV infection. J. Viral Hepat. *27*, 1096–1107.
20. Beudeker, B.J.B., van Oord, G.W., Arends, J.E., Schulze Zur Wiesch, J., van der Heide, M.S., de Knegt, R.J., Verbon, A., Boonstra, A., and Claassen, M.A.A. (2018). Mucosal-associated invariant T-cell frequency and function in blood and liver of HCV mono- and HCV/HIV co-infected patients with advanced fibrosis. Liver Int. *38*, 458–468.
21. Bolte, F.J., O'Keefe, A.C., Webb, L.M., Serti, E., Rivera, E., Liang, T.J., Ghany, M., and Rehermann, B. (2017). Intra-Hepatic Depletion of Mucosal-Associated Invariant T Cells in Hepatitis C Virus-Induced Liver Inflammation. Gastroenterology *153*, 1392–1403.e2.
22. Leeansyah, E., Ganesh, A., Quigley, M.F., Sönnerborg, A., Andersson, J., Hunt, P.W., Somsouk, M., Deeks, S.G., Martin, J.N., Moll, M., et al. (2013). Activation, exhaustion, and persistent decline of the antimicrobial MR1-restricted MAIT-cell population in chronic HIV-1 infection. Blood *121*, 1124–1135.
23. Wong, E.B., Akilimali, N.A., Govender, P., Sullivan, Z.A., Cosgrove, C., Pillay, M., Lewinsohn, D.M., Bishai, W.R., Walker, B.D., Ndung'u, T., et al. (2013). Low Levels of Peripheral CD161++CD8+Mucosal Associated Invariant T (MAIT) Cells Are Found in HIV and HIV/TB Co-Infection. PLoS One *8*, e83474.
24. Saeidi, A., Tien Tien, V.L., Al-Batran, R., Al-Darraji, H.A., Tan, H.Y., Yong, Y.K., Ponnampalavanar, S., Barathan, M., Rukumani, D.V., Ansari, A.W., et al. (2015). Attrition of TCR Va7.2+CD161++ MAIT Cells in HIV-Tuberculosis Co-Infection Is Associated with Elevated Levels of PD-1 Expression. PLoS One *10*, e0124659.
25. Freeman, M.L., Morris, S.R., and Lederman, M.M. (2017). CD161 Expression on Mucosa-Associated Invariant T Cells is Reduced in HIV-Infected Subjects Undergoing Antiretroviral Therapy Who Do Not Recover CD4+ T Cells. Pathog. Immun. *2*, 335–351.
26. Jouan, Y., Guillon, A., Gonzalez, L., Perez, Y., Boisseau, C., Ehrmann, S., Ferreira, M., Daix, T., Jeannet, R., François, B., et al. (2020). Phenotypical and functional alteration of unconventional T cells in severe COVID-19 patients. J. Exp. Med. *217*, e20200872.
27. Youngs, J., Provine, N.M., Lim, N., Sharpe, H.R., Amini, A., Chen, Y.-L., Luo, J., Edmans, M.D., Zacharopoulou, P., Chen, W., et al. (2021). Identification of immune correlates of fatal outcomes in critically ill COVID-19 patients. PLoS Pathog. *17*, e1009804.
28. Lu, B., Liu, M., Wang, J., Fan, H., Yang, D., Zhang, L., Gu, X., Nie, J., Chen, Z., Corbett, A.J., et al. (2020). IL-17 production by tissue-resident MAIT cells is locally induced in children with pneumonia. Mucosal Immunol. *13*, 824–835.
29. Sobkowiak, M.J., Davanian, H., Heymann, R., Gibbs, A., Emgård, J., Dias, J., Aleman, S., Krüger-Weiner, C., Moll, M., Tjernlund, A., et al. (2019). Tissue-resident MAIT cell populations in human oral mucosa exhibit an activated profile and produce IL-17. Eur. J. Immunol. *49*, 133–143.
30. Slichter, C.K., McDavid, A., Miller, H.W., Finak, G., Seymour, B.J., McNevin, J.P., Diaz, G., Czartoski, J.L., McElrath, M.J., Gottardo, R., and Prlic, M. (2016). Distinct activation thresholds of human conventional and innate-like memory T cells. JCI Insight *1*, e86292.
31. Chen, Z., Wang, H., D'Souza, C., Sun, S., Kostenko, L., Eckle, S.B.G., Meehan, B.S., Jackson, D.C., Strugnell, R.A., Cao, H., et al. (2017). Mucosal-associated invariant T-cell activation and accumulation after in vivo infection depends on microbial riboflavin synthesis and co-stimulatory signals. Mucosal Immunol. *10*, 58–68.
32. Hinks, T.S.C., Marchi, E., Jabeen, M., Olshansky, M., Kurioka, A., Pediongco, T.J., Meehan, B.S., Kostenko, L., Turner, S.J., Corbett, A.J., et al. (2019). Activation and In Vivo Evolution of the MAIT Cell Transcriptome in Mice and Humans Reveals Tissue Repair Functionality. Cell Rep. *28*, 3249–3262.e5.
33. Samer, C., Traves, R., Purohit, S.K., Abendroth, A., McWilliam, H.E.G., and Slobedman, B. (2021). Viral Impacts on MR1 Antigen Presentation to MAIT Cells. Crit. Rev. Immunol. *41*, 49–67.
34. Li, Y., Shi, C.W., Zhang, Y.T., Huang, H.B., Jiang, Y.L., Wang, J.Z., Cao, X., Wang, N., Zeng, Y., Yang, G.L., et al. (2022). Riboflavin Attenuates Influenza Virus Through Cytokine-Mediated Effects on the Diversity of the Gut Microbiota in MAIT Cell Deficiency Mice. Front. Microbiol. *13*, 916580.
35. Eberle, R.J., Olivier, D.S., Amaral, M.S., Pacca, C.C., Nogueira, M.L., Arni, R.K., Willbold, D., and Coronado, M.A. (2022). Riboflavin, a Potent Neuroprotective Vitamin: Focus on Flavivirus and Alphavirus Proteases. Microorganisms *10*, 1331.
36. Chancellor, A., Alan Simmons, R., Khanolkar, R.C., Nosi, V., Beshirova, A., Berloffa, G., Colombo, R., Karuppiah, V., Pentier, J.M., Tubb, V., et al. (2023). Promiscuous recognition of MR1 drives self-reactive mucosal-associated invariant T cell responses. J. Exp. Med. *220*, e20221939.
37. McSharry, B.P., Samer, C., McWilliam, H.E.G., Ashley, C.L., Yee, M.B., Steain, M., Liu, L., Fairlie, D.P., Kinchington, P.R., McCluskey, J., et al. (2020). Virus-Mediated Suppression of the Antigen Presentation Molecule MR1. Cell Rep. *30*, 2948–2962.e4.
38. Purohit, S.K., Samer, C., McWilliam, H.E.G., Traves, R., Steain, M., McSharry, B.P., Kinchington, P.R., Tscharke, D.C., Villadangos, J.A., Rossjohn, J., et al. (2023). Varicella zoster virus impairs expression of the non-classical major histocompatibility complex class I-related gene protein (MR1). J. Infect. Dis. *227*, 391–401.
39. Ashley, C.L., McSharry, B.P., McWilliam, H.E.G., Stanton, R.J., Fielding, C.A., Mathias, R.A., Fairlie, D.P., McCluskey, J., Villadangos, J.A., Rossjohn, J., et al. (2023). Suppression of MR1 by human cytomegalovirus inhibits MAIT cell activation. Front. Immunol. *14*, 1107497.
40. Roizman, B., Knipe, D.M., and Whitely, R.J. (2013). Herpes Simplex Viruses. In Fields Virology, 6th Edition, D.M. Knipe and P.M. Howley, eds. (Wolters Kluwer Health/ Lippincott Williams & Wilkins).
41. Hill, A., Jugovic, P., York, I., Russ, G., Bennink, J., Yewdell, J., Ploegh, H., and Johnson, D. (1995). Herpes-Simplex Virus Turns off the TAP to evade Host Immunity. Nature *375*, 411–415.
42. van Lint, A.L., Murawski, M.R., Goodbody, R.E., Severa, M., Fitzgerald, K.A., Finberg, R.W., Knipe, D.M., and Kurt-Jones, E.A. (2010). Herpes Simplex Virus Immediate-Early ICP0 Protein Inhibits Toll-Like Receptor 2-Dependent Inflammatory Responses and NF-kappa B Signaling. J. Virol. *84*, 10802–10811.
43. Wagner, L.M., Bayer, A., and DeLuca, N.A. (2013). Requirement of the N-Terminal Activation Domain of Herpes Simplex Virus ICP4 for Viral Gene Expression. J. Virol. *87*, 1010–1018.
44. Neumann, L., Kraas, W., Uebel, S., Jung, G., and Tampé, R. (1997). The active domain of the herpes simplex virus protein ICP47: A

potent inhibitor of the transporter associated with antigen processing (TAP). J. Mol. Biol. *272*, 484–492.
45. Oldham, M.L., Hite, R.K., Steffen, A.M., Damko, E., Li, Z., Walz, T., and Chen, J. (2016). A mechanism of viral immune evasion revealed by cryo-EM analysis of the TAP transporter. Nature *529*, 537–540.
46. Blees, A., Januliene, D., Hofmann, T., Koller, N., Schmidt, C., Trowitzsch, S., Moeller, A., and Tampé, R. (2017). Structure of the human MHC-I peptide-loading complex. Nature *551*, 525–528.
47. McWilliam, H.E.G., Mak, J.Y.W., Awad, W., Zorkau, M., Cruz-Gomez, S., Lim, H.J., Yan, Y., Wormald, S., Dagley, L.F., Eckle, S.B.G., et al. (2020). Endoplasmic reticulum chaperones stabilize ligand-receptive MR1 molecules for efficient presentation of metabolite antigens. Proc. Natl. Acad. Sci. USA *117*, 24974–24985.
48. Velusamy, T., Singh, N., Croft, S., Smith, S., and Tscharke, D.C. (2023). The expression and function of HSV ICP47 and its promoter in mice. J. Virol. *97*, e0110723.
49. Hill, A.B., Barnett, B.C., McMichael, A.J., and McGeoch, D.J. (1994). HLA class I molecules are not transported to the cell surface in cells infected with herpes simplex virus types 1 and 2. J. Immunol. (1950) *152*, 2736–2741.
50. York, I.A., Roop, C., Andrews, D.W., Riddell, S.R., Graham, F.L., and Johnson, D.C. (1994). A cytosolic herpes-simplex virus protein inhibits antigen presentation to CD8(+) T-lymphocytes. Cell *77*, 525–535.
51. McWilliam, H.E.G., Eckle, S.B.G., Theodossis, A., Liu, L., Chen, Z., Wubben, J.M., Fairlie, D.P., Strugnell, R.A., Mintern, J.D., McCluskey, J., et al. (2016). The intracellular pathway for the presentation of vitamin B-related antigens by the antigen-presenting molecule MR1. Nat. Immunol. *17*, 531–537.
52. Teo, C.S.H., and O'Hare, P. (2018). A bimodal switch in global protein translation coupled to eIF4H relocalisation during advancing cell-cell transmission of herpes simplex virus. PLoS Pathog. *14*, e1007196.
53. Elliott, G., and O'Hare, P. (1999). Live-cell analysis of a green fluorescent protein-tagged herpes simplex virus infection. J. Virol. *73*, 4110–4119.
54. Fox, H.L., Dembowski, J.A., and DeLuca, N.A. (2017). A Herpesviral Immediate Early Protein Promotes Transcription Elongation of Viral Transcripts. mBio *8*, e007455-17.
55. Bastian, T.W., Livingston, C.M., Weller, S.K., and Rice, S.A. (2010). Herpes Simplex Virus Type 1 Immediate-Early Protein ICP22 Is Required for VICE Domain Formation during Productive Viral Infection. J. Virol. *84*, 2384–2394.
56. Burch, A.D., and Weller, S.K. (2004). Nuclear sequestration of cellular chaperone and proteasomal machinery during herpes simplex virus type 1 infection. J. Virol. *78*, 7175–7185.
57. Adlakha, M., Livingston, C.M., Bezsonova, I., and Weller, S.K. (2020). The Herpes Simplex Virus 1 Immediate Early Protein ICP22 Is a Functional Mimic of a Cellular J Protein. J. Virol. *94*, e01564.
58. Bastian, T.W., and Rice, S.A. (2009). Identification of sequences in herpes simplex virus type 1 ICP22 that influence RNA polymerase II modification and viral late gene expression. J. Virol. *83*, 128–139.
59. Guo, L., Wu, W.-j., Liu, L.-d., Wang, L.-c., Zhang, Y., Wu, L.-q., Guan, Y., and Li, Q.-h. (2012). Herpes Simplex Virus 1 ICP22 Inhibits the Transcription of Viral Gene Promoters by Binding to and Blocking the Recruitment of P-TEFb. PLoS One *7*, e45749.
60. Zaborowska, J., Baumli, S., Laitem, C., O'Reilly, D., Thomas, P.H., O'Hare, P., and Murphy, S. (2014). Herpes Simplex Virus 1 (HSV-1) ICP22 Protein Directly Interacts with Cyclin-Dependent Kinase (CDK) 9 to Inhibit RNA Polymerase II Transcription Elongation. PLoS One *9*, e107654.
61. Fraser, K.A., and Rice, S.A. (2007). Herpes simplex virus immediate-early protein ICP22 triggers loss of serine 2-phosphorylated RNA polymerase II. J. Virol. *81*, 5091–5101.
62. Advani, S.J., Brandimarti, R., Weichselbaum, R.R., and Roizman, B. (2000). The disappearance of cyclins A and B and the increase in activity of the G2/M-phase cellular kinase cdc2 in herpes simplex virus 1-infected cells require expression of the α22/U(S)1.5 and U(L)13 viral genes. J. Virol. *74*, 8–15.
63. Orlando, J.S., Astor, T.L., Rundle, S.A., and Schaffer, P.A. (2006). The Products of the Herpes Simplex Virus Type 1 Immediate-Early US1/US1.5 Genes Downregulate Levels of S-Phase-Specific Cyclins and Facilitate Virus Replication in S-Phase Vero Cells. J. Virol. *80*, 4005–4016.
64. Zhang, M., Fu, M., Li, M., Hu, H., Gong, S., and Hu, Q. (2020). Herpes Simplex Virus Type 2 Inhibits Type I IFN Signaling Mediated by the Novel E3 Ubiquitin Protein Ligase Activity of Viral Protein ICP22. J. Immunol. (1950) *205*, 1281–1292.
65. Carter, K.L., and Roizman, B. (1996). The promoter and transcriptional unit of a novel herpes simplex virus 1 alpha gene are contained in, and encode a protein in frame with, the open reading frame of the alpha 22 gene. J. Virol. *70*, 172–178.
66. Hagglund, R., Munger, J., Poon, A.P.W., and Roizman, B. (2002). US3 Protein Kinase of Herpes Simplex Virus 1 Blocks Caspase 3 Activation Induced by the Products of US1.5 and UL13 Genes and Modulates Expression of Transduced US1.5 Open Reading Frame in a Cell Type-Specific Manner. J. Virol. *76*, 743–754.
67. Stanton, R.J., McSharry, B.P., Armstrong, M., Tomasec, P., and Wilkinson, G.W.G. (2008). Re-engineering adenovirus vector systems to enable high-throughput analyses of gene function. Biotechniques *45*, 659–662. 664-668.
68. Abós, B., Gómez Del Moral, M., Gozalbo-López, B., López-Relaño, J., Viana, V., and Martínez-Naves, E. (2011). Human MR1 expression on the cell surface is acid sensitive, proteasome independent and increases after culturing at 26 degrees C. Biochem. Biophys. Res. Commun. *411*, 632–636.
69. Everly, D.N., Feng, P., Mian, I.S., and Read, G.S. (2002). mRNA degradation by the virion host shutoff (Vhs) protein of herpes simplex virus: Genetic and biochemical evidence that Vhs is a nuclease. J. Virol. *76*, 8560–8571.
70. Feng, P., Everly, D.N., and Read, G.S. (2001). MRNA decay during herpesvirus infections: Interaction between a putative viral nuclease and a cellular translation factor. J. Virol. *75*, 10272–10280.
71. Taddeo, B., and Roizman, B. (2006). The virion host shutoff protein (U(L)41) of herpes simplex virus 1 is an endoribonuclease with a substrate specificity similar to that of RNase A. J. Virol. *80*, 9341–9345.
72. Feng, P., Everly, D.N., and Read, G.S. (2005). mRNA decay during herpes simplex virus (HSV) infections: Protein-protein interactions involving the HSV virion host shutoff protein and translation factors eIF4H and eIF4A. J. Virol. *79*, 9651–9664.
73. Shiflett, L.A., and Read, G.S. (2013). mRNA Decay during Herpes Simplex Virus (HSV) Infections: Mutations That Affect Translation of an mRNA Influence the Sites at Which It Is Cleaved by the HSV Virion Host Shutoff (Vhs) Protein. J. Virol. *87*, 94–109.
74. Riegert, P., Wanner, V., and Bahram, S. (1998). Genomics, isoforms, expression, and phylogeny of the MHC class I-related MR1 gene. J. Immunol. *161*, 4066–4077.
75. Lion, J., Debuysscher, V., Wlodarczyk, A., Hodroge, A., Serriari, N.E., Choteau, L., Ouled-Haddou, H., Plistat, M., Lassoued, K., Lantz, O., and Treiner, E. (2013). MR1B, a natural spliced isoform of the MHC-related 1 protein, is expressed as homodimers at the cell surface and activates MAIT cells. Eur. J. Immunol. *43*, 1363–1373.
76. Narayanan, G.A., Nellore, A., Tran, J., Worley, A.H., Meermeier, E.W., Karamooz, E., Huber, M.E., Kurapova, R., Tafesse, F.G., Harriff, M.J., and Lewinsohn, D.M. (2020). Alternative splicing of MR1 regulates antigen presentation to MAIT cells. Sci. Rep. *10*, 15429.
77. Friedel, C.C., Whisnant, A.W., Djakovic, L., Rutkowski, A.J., Friedl, M.-S., Kluge, M., Williamson, J.C., Sai, S., Vidal, R.O., Sauer, S., et al. (2021). Dissecting Herpes Simplex Virus 1-Induced Host Shutoff at the RNA Level. J. Virol. *95*, e01399-20.
78. Hennig, T., Djakovic, L., Dölken, L., and Whisnant, A.W. (2021). A review of the multipronged attack of herpes simplex virus 1 on the host transcriptional machinery. Viruses *13*, 1836.
79. Fenwick, M.L., and Everett, R.D. (1990). Inactivation of the shutoff gene (UL41) of Herpes-Simplex virus type-1 and type-2. J. Gen. Virol. *71*, 2961–2967.
80. Lim, H.J., Wubben, J.M., Garcia, C.P., Cruz-Gomez, S., Deng, J., Mak, J.Y.W., Hachani, A., Anderson, R.J., Painter, G.F., Goyette, J., et al. (2022). A specialized tyrosine-based endocytosis signal in MR1 controls antigen presentation to MAIT cells. J. Cell Biol. *221*, e202110125.
81. Harriff, M.J., Karamooz, E., Burr, A., Grant, W.F., Canfield, E.T., Sorensen, M.L., Moita, L.F., and Lewinsohn, D.M. (2016). Endosomal MR1 Trafficking Plays a Key Role in Presentation of Mycobacterium tuberculosis Ligands to MAIT Cells. PLoS Pathog. *12*, e1005524.
82. Berg, S., Kutra, D., Kroeger, T., Straehle, C.N., Kausler, B.X., Haubold, C., Schiegg, M., Ales, J., Beier, T., Rudy, M., et al. (2019). ilastik: interactive machine learning for (bio) image analysis. Nat. Methods *16*, 1226–1232.
83. Wertheim, J.O., Hostager, R., Ryu, D., Merkel, K., Angedakin, S., Arandjelovic, M., Ayimisin, E.A., Babweteera, F., Bessone, M., Brun-Jeffery, K.J., et al. (2021). Discovery of Novel Herpes Simplexviruses in Wild Gorillas, Bonobos, and Chimpanzees Supports Zoonotic Origin of HSV-2. Mol. Biol. Evol. *38*, 2818–2830.
84. Wertheim, J.O., Smith, M.D., Smith, D.M., Scheffler, K., and Kosakovsky Pond, S.L.

(2014). Evolutionary Origins of Human Herpes Simplex Viruses 1 and 2. Mol. Biol. Evol. *31*, 2356–2364.

85. Norberg, P., Tyler, S., Severini, A., Whitley, R., Liljeqvist, J.Å., and Bergström, T. (2011). A genome-wide comparative evolutionary analysis of herpes simplex virus type 1 and varicella zoster virus. PLoS One *6*, e22527.
86. Scherer, K.M., Manton, J.D., Soh, T.K., Mascheroni, L., Connor, V., Crump, C.M., and Kaminski, C.F. (2021). A fluorescent reporter system enables spatiotemporal analysis of host cell modification during herpes simplex virus-1 replication. J. Biol. Chem. *296*, 100236.
87. Johnson, K.E., Chikoti, L., and Chandran, B. (2013). Herpes Simplex Virus 1 Infection Induces Activation and Subsequent Inhibition of the IFI16 and NLRP3 Inflammasomes. J. Virol. *87*, 5005–5018.
88. Orzalli, M.H., Broekema, N.M., and Knipe, D.M. (2016). Relative Contributions of Herpes Simplex Virus 1 ICP0 and vhs to Loss of Cellular IFI16 Vary in Different Human Cell Types. J. Virol. *90*, 8351–8359.
89. Zhang, J., Wang, K., Wang, S., and Zheng, C. (2013). Herpes Simplex Virus 1 E3 Ubiquitin Ligase ICP0 Protein Inhibits Tumor Necrosis Factor Alpha-Induced NF-kappa B Activation by Interacting with p65/RelA and p50/NF-kappa B1. J. Virol. *87*, 12935–12948.
90. Huang, S., Gilfillan, S., Kim, S., Thompson, B., Wang, X., Sant, A.J., Fremont, D.H., Lantz, O., and Hansen, T.H. (2008). MR1 uses an endocytic pathway to activate mucosal-associated invariant T cells. J. Exp. Med. *205*, 1201–1211.
91. Treiner, E., Duban, L., Bahram, S., Radosavljevic, M., Wanner, V., Tilloy, F., Affaticati, P., Gilfillan, S., and Lantz, O. (2003). Selection of evolutionarily conserved mucosal-associated invariant T cells by MR1. Nature *422*, 164–169.
92. Gold, M.C., Cerri, S., Smyk-Pearson, S., Cansler, M.E., Vogt, T.M., Delepine, J., Winata, E., Swarbrick, G.M., Chua, W.J., Yu, Y.Y.L., et al. (2010). Human mucosal associated invariant T cells detect bacterially infected cells. PLoS Biol. *8*, e1000407.
93. Stelz, G., Rücker, E., Rosorius, O., Meyer, G., Stauber, R.H., Spatz, M., Eibl, M.M., and Hauber, J. (2002). Identification of two nuclear import signals in the alpha-gene product ICP22 of herpes simplex virus 1. Virology *295*, 360–370.
94. Poffenberger, K.L., Raichlen, P.E., and Herman, R.C. (1993). In vitro characterization of a herpes simplex virus type 1 ICP22 deletion mutant. Virus Gene. *7*, 171–186.
95. Orlando, J.S., Balliet, J.W., Kushnir, A.S., Astor, T.L., Kosz-Vnenchak, M., Rice, S.A., Knipe, D.M., and Schaffer, P.A. (2006). ICP22 Is Required for Wild-Type Composition and Infectivity of Herpes Simplex Virus Type 1 Virions. J. Virol. *80*, 9381–9390.
96. Sears, A.E., Halliburton, I.W., Meignier, B., Silver, S., and Roizman, B. (1985). Herpes simplex virus 1 mutant deleted in the alpha 22 gene: growth and gene expression in permissive and restrictive cells and establishment of latency in mice. J. Virol. *55*, 338–346.
97. Suzutani, T., Nagamine, M., Shibaki, T., Ogasawara, M., Yoshida, I., Daikoku, T., Nishiyama, Y., and Azuma, M. (2000). The role of the UL41 gene of herpes simplex virus type 1 in evasion of non-specific host defence mechanisms during primary infection. J. Gen. Virol. *81*, 1763–1771.
98. Pasieka, T.J., Lu, B., Crosby, S.D., Wylie, K.M., Morrison, L.A., Alexander, D.E., Menachery, V.D., and Leib, D.A. (2008). Herpes simplex virus virion host shutoff attenuates establishment of the antiviral state. J. Virol. *82*, 5527–5535.
99. Smith, T.J., Morrison, L.A., and Leib, D.A. (2002). Pathogenesis of herpes simplex virus type 2 virion host shutoff (vhs) mutants. J. Virol. *76*, 2054–2061.
100. Korom, M., Wylie, K.M., and Morrison, L.A. (2008). Selective ablation of virion host shutoff protein RNase activity attenuates herpes simplex virus 2 in mice. J. Virol. *82*, 3642–3653.
101. Su, C., and Zheng, C. (2017). Herpes Simplex Virus 1 Abrogates the cGAS/STING-Mediated Cytosolic DNA-Sensing Pathway via Its Virion Host Shutoff Protein. J. Virol. *91*, e02414–e02416.
102. Yokota, S.i., Yokosawa, N., Okabayashi, T., Suzutani, T., Miura, S., Jimbow, K., and Fujii, N. (2004). Induction of suppressor of cytokine signaling-3 by herpes simplex virus type 1 contributes to inhibition of the interferon signaling pathway. J. Virol. *78*, 6282–6286.
103. Shen, G., Wang, K., Wang, S., Cai, M., Li, M.L., and Zheng, C. (2014). Herpes Simplex Virus 1 Counteracts Viperin via Its Virion Host Shutoff Protein UL41. J. Virol. *88*, 12163–12166.
104. Zenner, H.L., Mauricio, R., Banting, G., and Crump, C.M. (2013). Herpes Simplex Virus 1 Counteracts Tetherin Restriction via Its Virion Host Shutoff Activity. J. Virol. *87*, 13115–13123.
105. Su, C., Zhang, J., and Zheng, C. (2015). Herpes simplex virus 1 UL41 protein abrogates the antiviral activity of hZAP by degrading its mRNA. Virol. J. *12*, 203.
106. Samady, L., Costigliola, E., MacCormac, L., McGrath, Y., Cleverley, S., Lilley, C.E., Smith, J., Latchman, D.S., Chain, B., and Coffin, R.S. (2003). Deletion of the virion host shutoff protein (vhs) from herpes simplex virus (HSV) relieves the viral block to dendritic cell activation: Potential of vhs(-) HSV vectors for dendritic cell-mediated immunotherapy. J. Virol. *77*, 3768–3776.
107. Tigges, M.A., Leng, S., Johnson, D.C., and Burke, R.L. (1996). Human herpes simplex virus (HSV)-specific CD8(+) CTL clones recognize HSV-2-infected fibroblasts after treatment with IFN-gamma or when virion host shutoff functions are disabled. J. Immunol. *156*, 3901–3910.
108. Trgovcich, J., Johnson, D., and Roizman, B. (2002). Cell surface major histocompatibility complex class II proteins are regulated by the products of the gamma(1)34.5 and U(L) 41 genes of herpes simplex virus 1. J. Virol. *76*, 6974–6986.
109. Wang, X., Hennig, T., Whisnant, A.W., Erhard, F., Prusty, B.K., Friedel, C.C., Forouzmand, E., Hu, W., Erber, L., Chen, Y., et al. (2020). Herpes simplex virus blocks host transcription termination via the bimodal activities of ICP27. Nat. Commun. *11*, 293.
110. Tormanen, K., Matundan, H.H., Wang, S., Jaggi, U., Mott, K.R., and Ghiasi, H. (2022). Small Noncoding RNA (sncRNA1) within the Latency-Associated Transcript Modulates Herpes Simplex Virus 1 Virulence and the Host Immune Response during Acute but Not Latent Infection. J. Virol. *96*, e0005422.
111. Seach, N., Guerri, L., Le Bourhis, L., Mburu, Y., Cui, Y., Bessoles, S., Soudais, C., and Lantz, O. (2013). Double Positive Thymocytes Select Mucosal-Associated Invariant T Cells. J. Immunol. *191*, 6002–6009.
112. Rouxel, O., Da Silva, J., Beaudoin, L., Nel, I., Tard, C., Cagninacci, L., Kiaf, B., Oshima, M., Diedisheim, M., Salou, M., et al. (2017). Cytotoxic and regulatory roles of mucosal-associated invariant T cells in type 1 diabetes. Nat. Immunol. *18*, 1321–1331.
113. Liu, Y., Zhu, P., Wang, W., Tan, X., Liu, C., Chen, Y., Pei, R., Cheng, X., Wu, M., Guo, Q., et al. (2021). Mucosal-Associated Invariant T Cell Dysregulation Correlates With Conjugated Bilirubin Level in Chronic HBV Infection. Hepatology *73*, 1671–1687.
114. Rawls, W.E., Laurel, D., Melnick, J.L., Glicksman, J.M., and Kaufman, R.H. (1968). A search for viruses in smegma, premalignant and early malignant cervical tissues. The isolation of herpesviruses with distinct antigenic properties. Am. J. Epidemiol. *87*, 647–655.
115. Schindelin, J., Arganda-Carreras, I., Frise, E., Kaynig, V., Longair, M., Pietzsch, T., Preibisch, S., Rueden, C., Saalfeld, S., Schmid, B., et al. (2012). Fiji: an open-source platform for biological-image analysis. Nat. Methods *9*, 676–682.
116. Schmittgen, T.D., and Zakrajsek, B.A. (2000). Effect of experimental treatment on housekeeping gene expression: validation by real-time, quantitative RT-PCR. J. Biochem. Biophys. Methods *46*, 69–81.

STAR★METHODS

KEY RESOURCES TABLE

REAGENT or RESOURCE	SOURCE	IDENTIFIER
Antibodies		
Mouse monoclonal anti-MR1-biotin (clone 26.5)	Jose Villadangos, The Peter Doherty Institute of Infection and Immunity, The University of Melbourne. McWilliam et al., 2016[51]	N/A
Human recombinant anti-HLA-ABC-PE (clone REA230)	Miltenyi Biotec	Cat#130-120-055; (RRID:AB_2751977)
Mouse monoclonal anti-MR1-PE (clone 26.5)	Biolegend	Cat#361105; RRID:AB_2563042
Mouse monoclonal anti-MR1-APC (clone 26.5)	Biolegend	Cat#361107; RRID:AB_2563204
Mouse monoclonal anti-HLA-ABC-APC (clone G46–2.6)	BD Biosciences	Cat#555555; RRID:AB_398603
Mouse monoclonal anti-HLA-ABC-SB436 (clone W6/32)	Invitrogen	Cat#62-9983-42; RRID:AB_2688263
Rabbit polyclonal Anti-MR1-CT, generated against the final 15 residues of human MR1 cytosolic tail (PREQNGAIYLPTPDR)	Jose Villadangos, The Peter Doherty Institute of Infection and Immunity, The University of Melbourne. McWilliam et al., 2016[51]	N/A
Mouse monoclonal anti-MR1	Abcam	Cat#ab55164; RRID:AB_944260
Mouse monoclonal anti-HLA-ABC (clone EMR8-5)	Abcam	Cat#ab70328; RRID:AB_1269092
Mouse monoclonal anti-GFP (clone B-2)	Santa Cruz Biotechnology	Cat#sc-9996; RRID:AB_627695
Rabbit polyclonal anti-GAPDH (FL-335)	Santa Cruz Biotechnology	Cat#sc-25778; RRID:AB_10167668
Rabbit monoclonal anti-DDDDK (clone EPR20018-251)	Abcam	Cat#ab205606; RRID:AB_2916341
Mouse monoclonal anti-HSV-1 ICP27 (clone RAd142)	Santa Cruz Biotechnology	Cat#sc-69806; RRID:AB_1124272
Mouse monoclonal anti-gD-FITC	Virostat	Cat#0196
Mouse monoclonal anti-gC-FITC	Virostat	Cat#0143
Goat polyclonal anti-adenovirus	Sigma-Aldrich	Cat#AB1056; RRID:AB_90213
Live/Dead™ Fixable blue	Invitrogen	Cat#L23105
Zombie NIR™ Fixable Viability Kit	Biolegend	Cat#423105
Streptavidin-PE	eBioscience	Cat#12-4317-87
Streptavidin-APC	eBioscience	Cat#17-4317-82
Wheat Germ Agglutinin CF405 M conjugate	Biotium	Cat#29028
Rabbit polyclonal anti-calreticulin	Sigma-Aldrich	Cat#C4606; RRID:AB_476843
Rabbit monoclonal anti-GM130 (clone D6B1)	Cell Signaling Technology	Cat#12480; RRID: AB_2797933
Rabbit monoclonal anti-EEA1 (clone F.43.1)	Invitrogen	Cat#MA514794; RRID:AB_10985824
Rabbit polyclonal anti-LAMP1	Abcam	Cat#ab24170; RRID: AB_775978
Donkey anti-Rabbit IgG (H + L) Highly Cross-Adsorbed Secondary Antibody, Alexa Fluor™ 546	Invitrogen	Cat#A10040
DAPI ready made solution	Sigma-Aldrich	Cat#MBD0015
Bacterial and virus strains		
HSV-1 Strain F	Dr Russell Diefenbach (Macquarie University)	Accession# GU734771
HSV-1 Strain 17	Prof Roger Everett (University of Glasgow)	Accession# NC_001806

(*Continued on next page*)

Continued

REAGENT or RESOURCE	SOURCE	IDENTIFIER
HSV-1 Strain KOS	Dr P Kinchington, Departments of Ophthalmology, and of Molecular Microbiology and Genetics, University of Pittsburgh	Accession# JQ780693
HSV-2 Strain 186	Dr Naomi Truong, The Westmead Institute for Medical Research. Rawls et al., 1968[114]	N/A
HSV-1 Strain 17 vhs mutant 17(41-)	Prof Roger Everett (University of Glasgow). Fenwick and Everett, 1990[79]	N/A
HSV-1 Strain KOS US12 mutant ICP47del	Velusamy et al., 2023[48]	N/A
SW102 *E. coli* containing the pAdZ5-C5 vector	Stanton et al., 2008[67]	N/A
5-alpha Competent *E. coli*	NEB	Cat#C2987H
Chemicals, peptides, and recombinant proteins		
Dulbecco's Modified Eagle's Medium	Lonza	Cat#12-604F
Hanks Balanced Salt Solution	Gibco	Cat#14170
Fetal Calf Serum	Cytiva	Cat#SH30084.02
Normal donkey serum	Sigma-Aldrich	Cat#D9663
Ac-6-FP Acetyl-6-formylpterin	Schircks	Cat#11.418
BD Cytofix™ Fixation buffer	BD Biosciences	Cat#554655
Folimycin (concanamycin A)	Sigma-Aldrich	Cat#C9705
MG132	Sigma-Aldrich	Cat#M7449
Fugene HD	Promega	Cat#E2231
Q5 High-Fidelity polymerase	NEB	Cat#M0491
Endo H	NEB	Cat#P0703S
DAB Substrate	Pierce	Cat#34065
BamHI-HF	NEB	Cat#R3136
SpeI-HF	NEB	Cat#R3133
BglII	NEB	Cat#R0144
XbaI	NEB	Cat#R0145
Xgal	Abcam	Cat#ab144388
IPTG	Abcam	Cat#ab142072
*Hind*III	NEB	Cat#R0104
T4 DNA ligase NEB	NEB	Cat#M0202
Geltrex™ basement membrane matrix	Gibco	Cat#A1413301
Critical commercial assays		
GFX™ PCR DNA and Gel Band Purification Kit	Cytiva	Cat#28903470
QIAprep Spin Miniprep Kit	QIAgen	Cat#27106X4
NucleoSpin® Gel and PCR Cleanup	Macherey-Nagal	Cat#740609
NucleoBond® Xtra Midi kit	Macherey-Nagal	Cat#740410
ISOLATE II RNA Mini Kit	Meridian Bioscience	Cat#BIO-52072
Affinity Script cDNA synthesis kit	Aligent Technologies	Cat#600559
Brilliant II SYBR Green qPCR Master Mix	Aligent Technologies	Cat#600828
Experimental models: Cell lines		
Human fibroblasts HF (male)	ATCC	SCRC-1041; RRID:CVCL_3285
Human ARPE-19 cell line (male)	ATCC	CRL-2302; RRID:CVCL_0145

(*Continued on next page*)

Continued

REAGENT or RESOURCE	SOURCE	IDENTIFIER
Human 293T cell line (female)	ATCC	CRL-3216; RRID:CVCL_0063
Human 293A cell line (female)	ATCC	Cat# 305070, RRID:CVCL_6910
Human T-REx™-293 cell line (female)	ThermoFisher	R71007; RRID:CVCL_D585
Green monkey Vero cell line (female)	ATCC	CCL-81; RRID:CVCL_0059
ARPE-19 MR1 (male)	McSharry et al., 2020[37]	N/A
ARPE-19 MR1-GFP (male)	McSharry et al., 2020[37]	N/A
Oligonucleotides		
HSV-1 F ICP22 pSY10-ICP22 Forward primer 5′- GTCTACACTAGTATGGCCGACAT TTCCCCAGG -3′	This study	N/A
HSV-1 F ICP22 pSY10-ICP22 Reverse primer 5′ GTCTACAGATCTCGGCCGGAGAA ACGTGTCGCTG -3′	This study	N/A
See Table S1. Primers used to amplify HSV-1 genes for recombination into pAdZ5-C5 vector	This study	N/A
See Table S2. Primers used for RT-qPCR, Related to STAR Methods.	This study	N/A
Recombinant DNA		
pSY10-ICP22	This study	N/A
pCDH_EF1-MCS-T2A-copGFP vector (pSY10)	Systems Bioscience, USA	Cat3#CD526A-1
pAdZ5-C5 (RAd-Ctrl)	Stanton et al., 2008[67]	N/A
RAd-ICP22	This study	N/A
RAd-US1.5	This study	N/A
RAd-vhs	This study	N/A
Software and algorithms		
FlowJo software, Version 10	Treestar Inc.	https://www.flowjo.com/
Paired Student's *t* tests or ANOVA analysis performed as indicated using Prism software, Version 10	GraphPad	https://www.graphpad.com/scientific-software/prism/
CLC Main Workbench, Version 22	QIAGEN	https://www.qiagenbioinformatics.com/products/clc-main-workbench/
ImageJ FIJI software, Version 1.53t	Schindelin et al., 2012[115]	https://imagej.net/software/fiji/
Ilastik software	Berg et al., 2019[82]	https://www.ilastik.org/

RESOURCE AVAILABILITY

Lead contact

Further information and requests for resources and reagents should be directed to and will be fulfilled by the Lead Contact, Barry Slobedman (barry.slobedman@sydney.edu.au).

Materials availability

Cells, viral mutants and constructs are available upon request, subject to our institutional and Material Transfer Agreements, and those with the host institution at which these reagents were generated.

Data and code availability

- All data reported in this paper will be shared by the lead contact upon request.
- This paper does not report original code.
- Any additional information required to reanalyze the data reported in this paper is available from the lead contact upon request.

EXPERIMENTAL MODEL AND STUDY PARTICIPANT DETAILS

Cells

Human fibroblasts HF, human retinal pigment epithelial (ARPE-19), 293T, 293A and ARPE-19 cell lines (all ATCC) expressing MR1 with co-expressed EGFP from the same promoter via a downstream internal ribosomal entry site or MR1-GFP, both under the control of the Murine stem cell virus LTR,[37] Vero (ATCC) and T-REx-293 (ThermoFisher) cells were grown at 37°C and 5% CO_2 in Dulbecco's Modified Eagle's Medium (Lonza) supplemented with 10% fetal calf serum (FCS, Cytiva). The sex of each cell line is listed in the key resources table. Cell lines have not been authenticated by ourselves.

Viruses

HSV-1 and HSV-2 strains used in this study were HSV-2 strain 186 (courtesy Dr Naomi Truong, The Westmead Institute for Medical Research),[114] HSV-1 strain F (courtesy Dr Russell Diefenbach, Macquarie University), HSV-1 17syn+ (Prof Roger Everett, University of Glasgow), HSV-1 17syn+ vhs mutant 17(41-) (Prof Roger Everett, University of Glasgow),[79] HSV-1 KOS (courtesy Prof P Kinchington, University of Pittsburgh) and US12 (ICP47) null mutant ICP47del.[48]

Cells were infected with HSV-1 or HSV-2 and mutant herpes viruses after replacing media for a 1 h period of adsorption (37°C), then washed and the media replaced. All HSV strains were grown and titrated on Vero cells.

Replication deficient adenovirus constructs were generated from the pAdZ5-C5 vector.[67] Adenoviruses used in this study were: RAd-Ctrl (no exogenous protein-coding region),[67] RAd-ICP22, RAd-US1.5, and RAd-vhs expressing the corresponding gene encoded by HSV-1 (strain F). Two-step PCR using Q5 High-Fidelity polymerase (NEB) was used to amply the viral genes adding either an N-terminal FLAG tag (US1 and US1.5) or a C-terminal V5 tag (UL41 gene), with the second round of amplification adding approximately 80 bp of homology to the vector construct. Primers are listed in Table S1, with the gene-specific sequence underlined. SW102 *E. coli* containing the pAdZ5-C5 vector were grown in low salt LB with ampicillin (50 μg/mL) at 32°C, shaking, until growth was exponential. Lambda red proteins were induced by incubation at 42°C for 15 min, cooled on ice for 15–20 min and centrifuged to isolate the cell pellet. The gel-purified PCR product was added to the competent SW102 cells which were electroporated in 0.2 cm cuvettes at 2.50 kV. After recovery in LB (32°C, shaking for 4 h) they were plated onto LB agar containing sucrose (5%), chloramphenicol (12.5 μg/mL), IPTG (200 μM) and Xgal (80 μg/mL) and then incubated for 30–48 h at 32°C. Several white colonies for each gene were selected for screening by incubating overnight (32°C, shaking) in LB containing chloramphenicol (12.5 μg/mL). DNA was purified (QIAgen) using 2-propanol to precipitate the DNA, before redissolving the DNA in 10 mM Tris pH 8.5. The sequence of each adenovirus insert was confirmed by Sanger sequencing and CLC Genomics workbench (QIAGEN).

Confirmed constructs were purified (Macherey-Nagel) and transfected into T-REx-293 cells using FuGene HD (Promega). After several days the infected cells were collected, and the pellet lysed by resuspending in equal volumes of PBS and tetrachloroethylene. After centrifugation the upper layer of PBS containing the adenovirus was removed and stored at −80°C. Virus was titrated after 48 h infection in T-REx-293 cells using goat anti-Adenovirus primary antibody (Sigma-Aldrich), anti-goat HRP secondary antibodies and DAB substrate (Pierce).

Plasmid expression constructs

Primers (Forward: 5′ GTCTAC**ACTAGT**ATGGCCGACATTTCCCCAGG 3′; reverse: 5′ GTCTAC**AGATCT**CGGCCGGAGAAACGTGTCGCTG 3′; US1 sequence underlined, restriction sites in bold) were used to amplify the HSV-1 (Strain F) US1 sequence excluding the stop codon with Q5 High-Fidelity polymerase (NEB). PCR products were purified and digested (SpeI-HF and BglII, NEB). The plasmid backbone (pCDH_EF1-MCS-T2A-copGFP vector, Systems Bioscience) was digested (XbaI and BamHI-HF, NEB), purified and ligated to the US1 fragment (NEB) to create the pSY10-ICP22 plasmid. This was transformed into 5-alpha *E. coli* (NEB), selected on LB agar with ampicillin (50 mg/mL) and purified (Macherey-Nagel). Sequence was confirmed by Sanger sequencing and CLC Genomics workbench (QIAGEN). 293T cells were transfected with 1 μg parental plasmid (pSY10) or pSY10-ICP22 using FuGene HD (Promega).

METHOD DETAILS

Quantitative reverse transcription polymerase chain reaction (qRT-PCR)

Total RNA was extracted (Meridian Bioscience) prior to cDNA synthesis and quantitative polymerase chain reaction (qPCR) (Aligent Technologies, Roche LightCycler480 Instrument II PCR machine). PCR settings were as follows: 10 min at 95°C for denaturation, then 45 amplification cycles of 30 s at 95°C, 40 s at 57°C and 20 s at 72°C, and the melt curve data was generated through 1 min at 95°C, 30 s at 50°C, 30 s at 95°C. Test gene mRNA levels were normalised to mRNA levels of the housekeeping gene 18s[116] using the ΔΔCT method. Primers used for RT-qPCR are listed in Table S2.

Immunoblotting

Cells were harvested in cell lysis buffer (50 mM NaCl, 50 mM TRIS pH8, 1% IGEPAL, 1% Triton X-100) supplemented with protease inhibitor cocktail (Sigma) and allowed to incubate on ice for 20 min. Lysates were then centrifuged (16,000 × g for 20 min at 4°C) and the supernatant collected. Lysates were mock or Endo H (NEB) digested according to the manufacturer's instructions for 90 min at 37°C as required. Lysates were denatured by heating at 95°C for 5 min in reducing sample buffer (Bio-Rad) and resolved by SDS- PAGE on precast polyacrylamide gels (Bio-Rad) before immunoblotting onto PVDF membranes. Membranes were probed with the designated primary antibodies in 3% BSA in PBST, followed by incubation with an appropriate horseradish peroxidase (HRP)-conjugated secondary antibody (all Santa Cruz

Biotechnology) and visualised using Clarity Western ECL Substrate (Bio-Rad). The following primary antibodies were utilised: anti-MR1 CT,[51] anti-MR1 (Abcam) and anti-HLA-A, B, C (Abcam), anti-GFP (Santa Cruz Biotechnology), anti-GAPDH (Santa Cruz Biotechnology or ThermoFisher), anti-DDDDK (anti FLAG, Abcam) and anti-ICP27 (Santa Cruz Biotechnology). Immunoblots depicted in Figures 2C and 3B are from the same experiment and depict the same Mock and RAd-Ctrl lanes. Unrelated samples were cropped from Figure 3B.

MR1 ligand and protein degradation inhibitors

The MR1 ligand Acetyl-6-formylpterin (Ac-6-FP 5 μM, Schircks Laboratories) was added as indicated to the culture medium. In the proteasomal and lysosomal inhibition assays, cells were treated with MG132 (5 μM, Sigma-Aldrich) or folimycin (50 nM Sigma-Aldrich) for 16 h prior to harvest.

Flow cytometry

The following antibodies were used to detect surface molecules: MHC-I by anti-HLA-A,B,C-PE (Miltenyi Biotec), anti-HLA-A,B,C-APC (BD Pharmingen) or anti-HLA,B,C-SB436 (Invitrogen), HSV-1 gD by anti-gD-FITC (Virostat) and HSV-1 gC by anti-gC (Virostat). Overexpressed MR1 was detected by anti-MR1 directly conjugated to PE or APC (Biolegend), while endogenous MR1 was detected by anti-MR1-biotin (clone 26.5,[51] followed by streptavidin conjugated to PE or APC (eBioscience). All cells were stained for 20–30 min at 4°C to minimise internalisation. Live cells were identified using Zombie NIR Fixable Viability Kit (Biolegend) or Live/Dead Fixable blue (Invitrogen). Cells were fixed after staining (BD Biosciences). Flow cytometry was performed using an LSR Fortessa X-20 or BD-LSR-II (BD Biosciences) and data analyzed using FlowJo software (Treestar Inc., https://www.flowjo.com, version 10.8).

Fluorescence imaging

ARPE-19 MR1-GFP cells were seeded in duplicate on 96 well PhenoPlates (PerkinElmer) precoated with Geltrex basement membrane matrix (Gibco) and then infected as described with either HSV-1, HSV-2 or adenovirus constructs. Cells were stained at 4°C for delineation of plasma membrane (Wheat Germ Agglutinin, CF405 M Conjugate Biotium) in Hanks Balanced Salt Solution (Gibco) with 2% normal donkey serum (Sigma-Aldrich). They were then fixed (BD Biosciences) and permeabilised and blocked with the staining buffer (phosphate buffered saline, 1 mM $CaCl_2$/$MgCl_2$, 2% NDS) containing either 0.01% saponin (Sigma-Aldrich) or for EEA1 staining 0.01% Triton X-100 (Sigma-Aldrich). The following primary rabbit anti-human antibodies were used to label intracellular compartments: calreticulin for the ER (Sigma-Aldrich), GM130 for the Golgi apparatus (Cell Signaling Technology), EEA1 for early endosomes (ThermoFisher) and LAMP1 for late endosomes/lysosomes (Abcam). This was followed by Donkey anti-Rabbit IgG conjugated to Alexa Fluor 546 (ThermoFisher) and DAPI nuclear staining (Sigma-Aldrich). Cells were washed several times between each staining step and then covered in degassed imaging buffer (5% (v/v) Glycerol, 2.5% (w/v) DABCO Powder in PBS, pH 8.5). GFP was used to identify the location and signal strength of the MR1-GFP construct. Two biological repeats were completed for each set of assay conditions.

Cells were imaged using the Opera Phenix Plus (PerkinElmer) with the 40X water objective, under control of the Harmony software. A minimum of 4 fields of view (FOV) were imaged per well, with five planes, each 0.5 μm apart, acquired in each channel. Maximum z stack projections were created for each FOV and flat field correction was applied through ImageJ FIJI software.[115] A segmentation map of the cells within each FOV defining the subcellular compartments was created with ilastik software.[82] After normalising the median MR1-GFP FOV signal to the control samples within the corresponding experimental condition, the median MR1-GFP signal at each subcellular location was calculated with ImageJ by overlaying the segmentation map. Fold change in the median MR1-GFP signal in the FOV at each subcellular compartment in infected cells compared to corresponding mock infected or RAd-Ctrl infected samples was calculated. In addition, the median MR1-GFP signal within each FOV was used to calculate the relative strength of GFP signal restricted to the subcellular compartment compared to the median cell signal. Statistical significance was evaluated with a minimum of 14 FOV.

QUANTIFICATION AND STATISTICAL ANALYSIS

Paired Student's t tests, Welch's unpaired t-test, or ANOVA analyses were performed, as indicated in each figure legend, using GraphPad Prism software (LLC). Data are presented as dot plots (flow cytometry and RT-qPCR) with the mean ± SEM, or violin plots (fluorescence microscopy) with the median and quartiles. Statistical significance is represented as *$p < 0.05$, **$p < 0.005$, ***$p < 0.0005$, or ****$p < 0.0001$. Number of experimental repeats (flow cytometry, RT-qPCR and fluorescence microscopy) and independent FOV (fluorescence microscopy) are indicated in each figure legend.